Mechanisms of neurotransmitter receptor packaging and delivery to the synapse.

Inauguraldissertation

zur

Erlangung der Würde eines Doktors der Philosophie

vorgelegt der

Philosophisch-Naturwissenschaftlichen Fakultät

Universität Basel

Von

Michael Abanto

Aus New Jersey, USA

Basel 2014

Genehmigt von der Philosophisch-Naturwissenschaftlichen Fakultät auf Antrag von:

Prof. Dr. Pico Caroni
(Dissertationsleiter)

Prof. Dr. Peter Scheiffele
(Korreferent)

Basel, den 26.06.2012

Prof. Dr. J. Schibler
(Dekan)

Table of Contents

Abbreviations.

ACh	acetylcholine
AChR	acetylcholine receptor
AMPAR	(2-amino-3-(5-methyl-3-oxo-1,2- oxazol-4-yl)propanoic acid receptor
ANOVA	analysis of variance
BTX	bungarotoxin
BTX-488	bungarotoxin conjugated to a fluorophore (peak excitation at 488nm)
Cav-3/cv3	caveolin-3
CNS	central nervous system
DMEM	Dulbecco's modified Eagle's medium
DTB	detubulation
Dysf	dysferlin
Dystro	dystroglycan
ECM	extracellular matrix
ER	endoplasmic reticulum
FRAP	flouresence recovery after photobleaching
GABAR	gamma-aminobutyric acid receptor
GFP	green fluorescent protein
GlyR	glycine receptor
Glur1	AMPAR subunit 1
Glur2	AMPAR subunit 2
MTM1	myotubularin
NCAM	neural cell adhesion molecule
NMDAR	N-Methyl-D-aspartic acid
PNS	peripheral nervous system
PSD	postsynaptic density
QDT	quantum dot
SA	spine apparatus
SEM	standard error of the mean
TGN	transgolgi network

Acknowledgements.

I would like to thank my supervisor, Pico Caroni, for giving me the opportunity to work in his lab. Pico encouraged my imagination, but also made me practical.

I am grateful for my committee, Peter Scheiffele and Jan Pielage, for their advice and interesting ideas over the many years.

It is most important that I acknowledge the Caroni lab over the last 6 years. Discussions at PR, in the lab, and over a coffee composed a large portion of my scientific and personal joy during my stay at the FMI. I must first thank Ewa Bednarek for encouraging me to do a PhD, and move to the Caroni lab. I thank Nadine Gogolla and Ivan Galimberti, for easing me into the lab. Tamara Brown introduced me to the C2C12 system and made the original observation that endocytosis might be involved in clustering. Yuichi Deguchi taught me all there is to know about 1) human methods for gravitation chromosomal sorting, and 2) where the mouse house really is. Flavio Donato expanded my thought and sense of humor, in every direction. I am similarly indebted to Dr. Francois Grenier, a titan of neuroscientific thinking and endless friend.

Thanks to my L.T.s. Morning.

My parents and brothers encouraged me to do anything and everything from rugby to neuroscience, and they gave me the ability to go anywhere, do anything, and be happy. Thanks Mom, Dad, Bryan, Damon, and Anthony.

Summary.

During development and learning, synapses increase their strength by adding neurotransmitter receptors to the postsynapse. The current model of postsynaptic receptor addition is the 'diffusion-trap'. In this model, receptors insert extrasynaptically and then diffuse into the postsynapse, where they are trapped via interaction with scaffold molecules. Here we propose a new model for postsynaptic receptor addition: the 'preassemble-insert' model. In this model, extrasynaptic receptors endocytose, preassemble with scaffold, and then insert directly to the postsynapse without a diffusion step. Hence receptor-scaffold packages are inserted as immobile units in the postsynapse.

To investigate postsynaptic receptor diffusion-trapping and preassembly-insertion, we use the agrin model of AChR clustering, live cell imaging, FRAP, and single molecule tracking. We find that AChRs diffuse into clusters during formation, but directly insert during strengthening. Inserted AChRs transcytose from the surface plasma membrane via caveolin-3 t-tubules, and then exocytose via a Rab27a vesicular compartment, in a MyosinVa dependant manner. During caveolin-3 t-tubule transcytosis, AChRs preassemble with the scaffold molecule rapsyn in a transport package, and caveolin-3 trafficking is required for AChR-rapsyn packaging. Insertion of preassembled AChR-rapsyn packages is required for AChR cluster strengthening, but not formation.

α Dystroglycan does not preassemble with AChR-rapsyn, and clusters independently of the caveolin-3 t-tubule pathway. However, α dystroglycan is required for caveolin-3 t-tubule organelle recruitment and polarization towards the cluster, which permits the insertion of AChR-rapsyn packages. Finally, we confirm caveolin-3 and Rab27a trafficking in vivo, and correlate t-tubule recruitment with NMJ strengthening. We also report prepackaging of Glur1-stargazin at CNS synapses after chemical LTP.

The ‘diffusion-trap’ has predominated as the model for postsynaptic receptor addition, and is a generalized mechanism for the addition of transmembrane protein to cell-cell junctions. These findings provide evidence for a new model of postsynaptic receptor addition, in which preassembled protein complexes insert directly, without a diffusion step.

Introduction.

In this thesis I present evidence for the preassembly of receptor-scaffold complexes inside a calcium handling organelle (the t-tubules), followed by insertion of immobile receptor-scaffold complexes. Hence I will introduce what is known about receptor trafficking, mobility, and complex assembly at the postsynapse, as well as what is known about postsynaptic calcium handling organelles like t-tubules and ER. Finally I will highlight agrin-induced AChR clustering as an experimental model to investigate receptor trafficking and packaging.

Diffusion-trapping of receptors at the postsynapse.

The postsynaptic addition of neurotransmitter receptors strengthens synsapses and is an important trafficking event in development and learning. The 'diffusion-trap' is the primary model for postsynaptic addition, involving 1) extrasynaptic receptor insertion, 2) receptor diffusion into the postsynapse, and 3) receptor trapping via receptor-scaffold interaction (fig 1.1)(Opazo and Choquet 2011). Evidence for this diffusion-trap model has been found throughout excitatory and inhibitory synapses in the central and peripheral nervous systems (AMPARs, NMDARs, AChR, GlyR, GABARs, (reviewed in Renner et al 2008). Furthermore, diffusion-trapping occurs during a wide range of processes including synapse formation, strengthening, maintenance, and plasticity (Renner et al 2008).

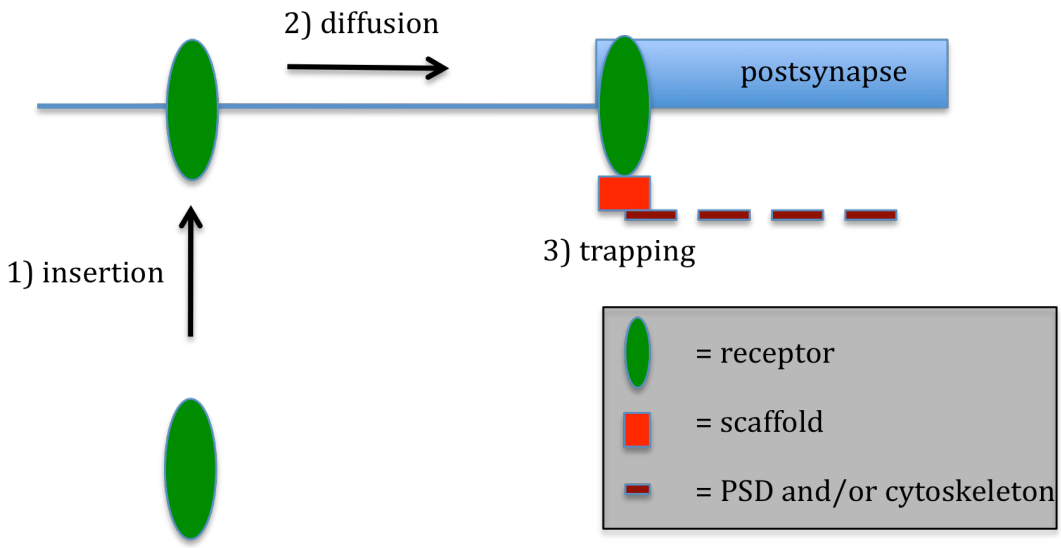

Figure 1.1 The diffusion-trap model.
In the three-step model, receptors (green oblongs) 1) insert extrasynaptically, 2) diffuse into the synapse, and 3) trap in the synapse by receptor-scaffold-PSD interaction.

The diffusion-trap hypothesis originated from AChR clustering experiments over 35 years ago (Axelrod et al 1976), and has been verified many times since. In these original experiments, AChRs were labeled with bungarotoxin conjugated to a fluorophore and the fluorescence recovery after photobleaching (FRAP) was measured at clusters. AChR diffusion was implied by a fast recovery of fluorescence, on the order of seconds to minutes.

The advent of GFP, sophisticated fluorophores like quantum dots, and better microscopes has revolutionized the study of receptor trafficking. Now it is possible to image individual receptors diffusing into a synapse, rather than extrapolating diffusion from FRAP data, and it also possible to image the exocytosis of single vesicles. Much of the current knowledge about postsynaptic receptor trafficking comes from work on Glur1 in the CNS, and AChR in the PNS, which are highlighted throughout this introduction.

There are two possible trafficking routes to the synapse, insertion from an intracellular compartment or diffusion from a surface pool. A direct comparison of insertion versus diffusion has been made using a pH sensitive GFP tagged to Glur1 in

organotypic slices (Makino and Malinow 2009). This study found Glur1 inserted into the dendritic shaft after LTP induction, and that the majority of receptors added to the synapse were from a surface pool. In the model from this paper, extrasynaptic insertion facilitates postsynaptic receptor addition only by adding to the pool of available receptors that can diffuse into the synapse. High-resolution imaging also confirmed Glur1 insertion at the dendritic shaft, and that inserted receptors diffused into the synapse (Yudowski et al 2007).

Single molecule tracking of AMPARs with quantum dots (QDT) also supports the classical diffusion-trap model. QDTs enable single molecule tracking because they are extremely bright, difficult to bleach, and can be conjugated to streptavidin or antibodies (Triller and Choquet 2008). Surface GluR1-QDTs have been shown to diffuse into synapses after LTP induction in vitro, and then become immobile in the synapse (Opazo et al 2010). This process depends on Camk2 phosphorylation of the Glur1 auxiliary protein, stargazin. In turn, phosphorylated stargazin increases it's affinity for PSD95, which anchors and immobilizes the receptor in the synapse via the Glur1-stargazin-PSD95 link. Hence the GluR1-stargazin complex is mobile outside the synapse, while Glur1-stargazin-PSD95 is immobile in the synapse (fig 1.2).

Similar experiments with QDTs have found evidence for diffusion-trapping for every receptor studied (NR2a, NR2b, the AMPARs, GlyR, GabaRs, AChRs, and more) (reviewed in Triller and Choquet 2003 and 2008). Like Glur1-stargazin, many receptors are trapped in, or anchored to, the PSD via an intermediate scaffold molecule after a stimulus induction, which leads to a decreased mobility or even immobility in the postsynapse. In other words, the degree to which receptor-scaffold-PSD complexes are assembled determines receptor mobility in the synapse, and complex assembly is inducible. After agrin-induced phosphorylation, AChRs increase their affinity for the scaffold molecule rapsyn, increasing the number of bound rapsyns per AChR from 1 to 2 (Moransard et al 2003). This AChR-2x(rapsyn) complex is correlated with increased AChR stability in the postsynapse (Gervasio et

al 2007)(fig 1.2). Similarly, the affinity of glycine receptors (GlyR) for the scaffold molecule gephyrin increases after NMDAR stimulation to regulate diffusion trapping (Levi et al 2008), and diffusing GABARs also trap more at synapses via gephyrin after electrical stimulation, in a calcium and calcineurin dependent manner (Jacob et al 2005, and Bannai et al 2009). Hence receptor-scaffold interaction can be dynamically modulated to control receptor mobility or anchorage in the synapse.

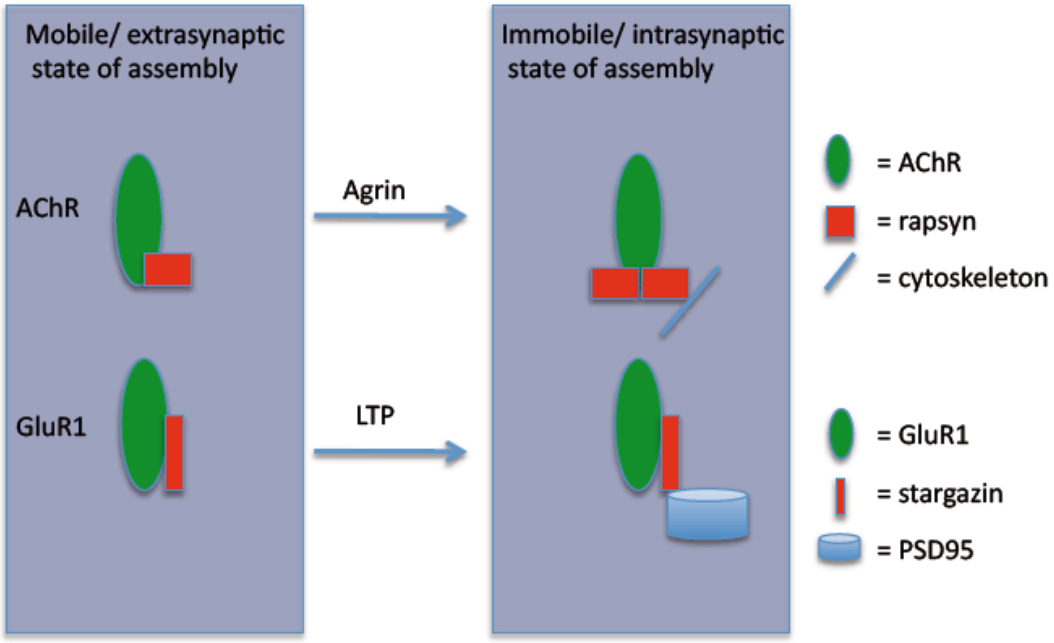

Figure 1.2 States of assembly that correlate with receptor mobility and immobility. Left, extrasynaptic receptors are constitutively bound to a linker or scaffold molecule, and the complex is highly mobile outside the synapse. Right, stimulation by agrin or LTP induces the formation of a receptor-scaffold-cytoskelton/PSD complex, which is trapped immobile in the postsynapse. Hence the state of receptor assembly correlates with receptor mobility. In the upper right, there are two rapsyns per AChR, in the immobile state of assembly. A similar increase in ratio may also occur between Glur1 and stargazin.

This induced receptor-scaffold assembly is assumed to happen and be regulated locally at the synapse, after diffusion into the postsynapse (Opazo and Choquet 2011). However whether receptor-scaffold interaction occurs at or very near the synapse has not been determined. There have been reports of extrasynaptic GlyR already assemble with the scaffold gephyrin (Ehrensperger et al 2007), and these preassembled complexes were still mobile in the membrane. Similarly AChRs are constitutively bound to one rapsyn, and Glur1-stargazin complex is also preformed.

However phosporylation can change the affinity of the scaffold molecule for PSD, as in Glur1-stargazin (Opazzo et al 2010), or add more scaffold per receptor as is the case for AChR-rapsyn (Moransard et al 2003), and potentially Glur1-stargazin (Shi et al 2009). In summary there are a variety of ways to alter receptor-scaffold, or receptor-scaffold-PSD, interactions. This interaction is thought to be regulated locally at the synpase by phosphorylation, even if receptors are already preassembled with scaffold. However, I will later introduce evidence which suggests that receptor-scaffold complexes might preassemble remotely, before arriving at the synapse.

There are several other modes of synaptic receptor trapping, such as direct receptor-PSD interaction, ECM modulation, cell adhesion molecule interaction, interaction with other neurotransmitter receptors, the lipid composition and viscosity of the membrane, the number and density of other immobile and clustered proteins, and more, but they will not be considered here (but are reviewed in Triller and Choquet 2003).

Insertion.

While there have been very many examples of diffusing receptors becoming trapped in synapses, few other models for postsynaptic receptor addition have been proposed. Surface receptor insertion is always prerequisite for surface diffusion into the synapses, and insertion is regulated during development and plasticity. Hence the role of insertion in diffusion-trap models is to increase the surface pool of receptors that can diffuse and trap. However, some studies have proposed direct postsynaptic insertion without a diffusion step. The questions of whether receptors can insert directly into the postsynapse, and whether directly inserted receptors

diffuse or are immobile, remain open (fig 1.3).

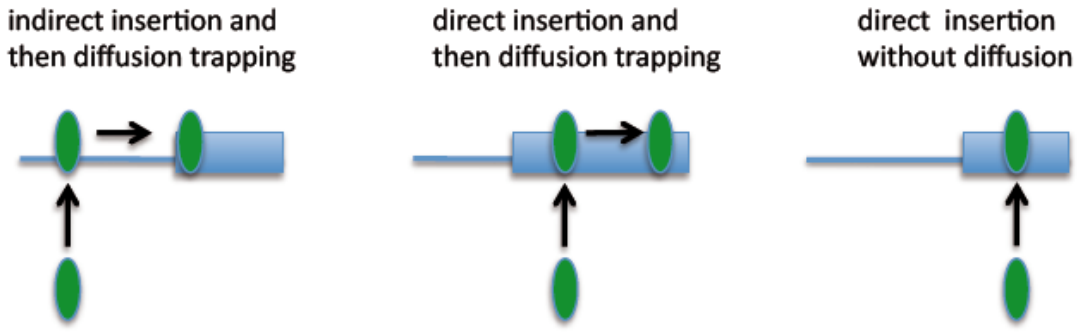

Figure 1.3 Three possible modes of insertion.
Left, receptors insert extrasynaptically, diffuse, and then trap. Middle receptors are inserted intrasynaptically, diffuse, and then trap. Right, receptors insert intrasynaptically as immobile units.

The question of insertion versus diffusion has been addressed in an AChR clustering model in vitro, with a chick myotube-axon co-culture (Dubinsky et al 1989). Consistent with many reports, the authors found surface AChR diffusion into clusters. However, after clusters formed, receptors inserted directly into the middle of clusters, rather than at the periphery or elsewhere in the membrane. Furthermore, inserted receptors were immobile, as were receptors trapped after diffusion. Whether inserted receptors were inserted immobile or first diffused and then trapped within clusters is uncertain.

The authors also proposed that there must be a mechanism to regulate the direct insertion of AChRs to clusters. Recent data demonstrates receptor insertion at AChR clusters, in xenopus muscle in vitro, mediated by cofilin (Lee et al 2009). However, in this animal model, AChRs were found to be mobile within the cluster after insertion, and the sites of insertion were considered intrasynaptic perforations, rather than veritable PSD. Hence there is little data on direct insertion, and whether or not inserted receptors are mobile or immobile is uncertain (fig 1.3), based on the two studies mentioned.

Both of these papers demonstrate direct postsynaptic AChR insertion. Both papers allow the possibility of intermediate diffusion after insertion, but the former paper

presents the possibility that AChRs insert immobile, without a diffusion step. However, it is technically very difficult to demonstrate that immobile insertion happens without any diffusion. Ultimately, a demonstration of immobile insertion would require single molecule imaging of insertion, which is the approach in this thesis.

There is some experimental evidence that Glur2 inserts directly into synapses (Passafaro et al 2001). In contradiction, single molecule tracking has also shown Glur2s diffusing into synapses (Tardin et al 2003). Without single-molecule tracking of insertion it is difficult to exclude diffusion and demonstrate direct immobility. Beyond Glur2, there is no suggestion or reports of other neurotransmitters inserting directly into synapses without a diffusion step.

Unexpectedly, direct insertion of connexins does occur at gap junctions, the electrical synapse. Connexins were previously thought to insert extrasynaptically and then diffuse into the synapse, until recent evidence for direct insertion was produced (Shaw et al 2007). That connexins insert directly, rather than diffuse in from the periphery, was an important paradigm shift for gap junction and synapse trafficking.

While the imaging of single molecule diffusion in the membrane is now relatively common, imaging of single molecule insertion remains elusive, and the imaging of single vesicle exocytosis at the postsynapse is rare. Super-resolution, and single molecule imaging studies have revealed important insights into presynaptic vesicle fusion (Willig et al 2006) and receptor trafficking in live cells (Triller and Choquet 2008). There are few postsynaptic studies imaging single postsynaptic vesicle exocytosis events, and the results have been contradictory. Some groups have shown baseline and plasticity induced insertion of AMPARs in the dendritic shaft and not at the synapse, in vitro (Yudowski et al 2007 and Makino and Malenka 2009). On the other hand there is new evidence for insertion directly into spines

(Patterson et al 2010), and evidence of a perisynaptic exocytic hotspot (Kennedy et al 2010).

Direct insertion at the synapse, and insertion of an immobile receptor, are both possible, but there is not strong evidence, yet, for these possibilities. Single molecule tracking of inserted receptors would be required to distinguish direct insertion of an immobile receptor form direct insertion followed by short diffusion and then immobility. Hence single molecule tracking of inserted receptors is an approach taken in this thesis.

Receptor-scaffold prepackaging.

The assembly of the postsynaptic complex is a difficult task because there are hundreds of molecules with precise stoichiometries in the PSD (Sheng and Hoogenraad 2007). To what degree molecular complexes assemble locally at the postsynapse, versus remotely, is still being elucidated. In the context of the diffusion-trap mechanism described above, it is thought that receptor-scaffold-PSD complexes form locally, after receptors diffuse into the postsynapse (e.g. AChR-rapsyn-cytoskeleton, or Glur1-stargazin-PSD95). However, recent data has shown receptor-scaffold-PSD preassembly, in vesicular 'transport packages', before arriving at the synapse.

The NMDA receptor has been shown to preassemble with SAP102, a PSD-95 related molecule, before arriving at the synapse. Preassembled NMDAR-SAP102 packages traffic in recycling vesicles, or 'transport packages' (Washbourne et al 2002), and SAP102 interacts with sec8, targeting packages for membrane insertion (Sans et al 2003). NMDARs were also shown to prepackage with CASK and SAP97 (Jeyifous et al 2007). Hence there is evidence that receptors can preassemble with scaffold inside the cell, before arriving at the synapse. However, how the NMDAR-scaffold complex relates to receptor mobility is not known.

Whether other receptors prepackage with scaffold, whether prepackaging can be induced or dynamically regulated, or if prepackaging influences receptor mobility and stability in the synapse is unknown. It should also be noted that the NMDAR prepackaging model has also been contradicted (Bresler et al 2004), and evidence of other postsynaptic receptor transport packages is lacking.

Prepackaging in and of itself is not the sole focus of this study. The important question to address is whether the receptor-scaffold state of assembly, which is correlated with receptor immobility, is regulated locally at the synapse, or remotely, such as inside transport vesicles. Furthermore, it will be important to address whether preassembly is causally related to receptor immobility.

I previously suggested the possibility of direct insertion of immobile receptors at the postsynapse. Because receptor immobility is tightly correlated with receptor-scaffold-PSD complex assembly, a preassemble-insert mechanism might be required for the direct insertion of immobile receptors. In a preassemble-insert model, the state of assembly (receptor-scaffold-PSD) would be determined remotely in the cell, in transport packages (fig 1.4). This is in contrast to a diffusion trap model, where the assembly would happen at the synapse surface after the receptor diffuses in, as a sort of 'post packaging' or anchoring in situ (fig 1.1). For AChRs preassembly-insertion would predict intracellular vesicles with two rapsyns per AChR (as schematically depicted in fig 1.4), and for GluR1 this could mean more stargazin per GluR1 or a GluR1-stargazin-PSD-95 assembly.

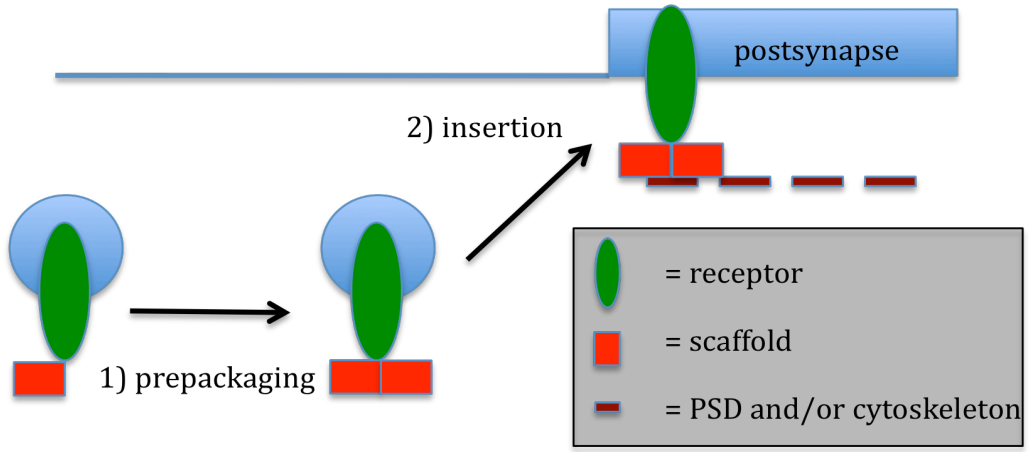

Figure 1.4 The preassemble-insert model.
In this model, intracellular receptors (green oblongs inside vesicles, blue circles) are 1) packaged with scaffold, and 2) inserted directly into the postsynapse as an immobile receptor-scaffold package. Two scaffold molecules (red) are present after prepackaging to represent twp rapsyn scaffold molecules per AChR.

Relatively little is known about preassembly and insertion of immobile receptor complexes. For example if preassembly occurs, does it occur in the synthetic pathway, or is it induced after stimulus? Furthermore, what organelle traffics and assembles receptor complexes is unknown. Below I will propose that calcium handling organelles, like ER and t-tubules, are possible candidates to traffic and preassemble receptor complexes.

Postsynaptic recruitment of endoplasmic reticulum and its derivatives.

During development and plasticity, receptor number, receptor mobility, and receptor-scaffold interaction are not the only variables changing at the postsynapse. Intracellular organelles like smooth endoplasmic reticulum (ER), spine apparatus (SA), and t-tubules are also recruited. The roles of postsynaptic ER in synaptic function are unclear, but thought to involve regulation of local calcium concentration; transmission of calcium signal over long distance; contribution to postynaptic or endosomal membrane; and local protein synthesis (reviewed in Ramirez and Couve 2010).

While little is known about postsynaptic ER function, there are some clues that suggest an involvement with receptor trafficking and perhaps plasticity. For example, receptors have been localized to postsynaptic and dendritic ER. AMPARs and NMDARs have been found inside SA and spine ER, but how they trafficked there and what they do there is unknown (Racca et al 2000). NMDARs have also been found packaged with SAP97 and CASK in dendritic ER (Jeyifous et al 2007). Whether this packaging or any packaging occurs at postsynaptic ER is unknown. It has also been reported that the ER responds to plasticity. Spine ER reacts to NMDAR dependent plasticity in vitro by fragmenting (Kucharz et al 2009), and loss of spine ER in synaptopodin knockout mice results in impaired theta oscillation induced LTP and memory deficit in vivo (Jedlicka et al 2009 and Deller et al 2003). Hence little is known about postsynaptic ER function but it might traffic receptors, and have a role in plasticity.

More concretely, postsynaptic ER recruitment correlates with synaptic strength. Postsynaptic ER is selectively recruited to a subset of large mature spines, which have particularly strong synapses compared to spines without ER, in hippocampal CA1 (Holbro et al 2009). 'Strength' of the postsynapse, in this case, correlates with spine size but is also defined by a larger excitatory postsynaptic current (EPSC). Why some spines recruit ER or SA and others do not is unknown.

Approximately 20% of hippocampal, lateral amygdala, and neocortical spines have SA or ER. Despite this sparseness, ER/SA spines have interesting functions. They contribute a stronger excitatory drive and have larger EPSCs compared to spines without ER (Holbro et al 2009). Spines that are stable in vivo for days or weeks contain ER (Knott et al 2006), and such stable, ER rich spines also disappear after sensory deprivation (Holtmaat et al 2006). Finally, after fear conditioning, the fraction of spines with SA increases in the lateral amygdala (Ostroff et al 2010), which implies that recruitment of ER spines is inducible, or that new ER rich spines are added.

The above exemplifies recruitment of ER, or its SA derivative, to specific subpopulations of postsynapses. However, some synapses have been reported to invariably recruit postsynaptic ER, and these synapses are also known to be remarkably strong. This includes ER/SA recruitment the mossy fiber synapse in the hippocampus (Orth et al 2005), the purkinje cells in the cerebellum (Martone et al 1993), and an ER connected organelle called 't-tubules' at neuromuscular junctions (Hezel et al 2010). T-tubules and spine ER or SA are similar in their ability to propagate calcium signals.

T-tubules have been well studied for their role in propagating calcium signals throughout the muscle after depolarization at the NMJ. However, unlike other ER derivatives, they are also known to have a role in membrane protein trafficking. Throughout the muscle, t-tubules are involved in membrane repair and fusion, mediated by dysferlin (a t-tubule specific trafficking protein)(Glover and Brown 2007). Caveolin-3 is a muscle specific caveolin, involved in dysferlin mediated membrane repair and muscle caveolar endocytosis. Myotubularin (MTM1) is a lipid phosphatase thought to regulate lipid content and receptor trafficking at early and late endosomes (Cao et al 2008). These t-tubule proteins are clearly involved in trafficking, though precisely how they work is still being elucidated. Whether they are involved in receptor-scaffold packaging and trafficking, or any synaptic trafficking, is unknown.

Although it is not understood how ER organelles or t-tubules might be postsynaptically recruited, there is some data on other postsynaptic organelle recruitment. Cell adhesion is known to play a role in postsynaptic recruitment of the transgolgi network (TGN). For example, neural cell adhesion molecule (NCAM) is recruited to axo-dendritic contacts in early synapse formation, and can recruit the TGN. Before synaptogenesis, NCAM forms a link with the TGN organelle, via spectrin (Sytnyk et al 2002), and therefore NCAM-TGN packages are recruited to forming synapses.

Whether cell adhesion regulates the postsynaptic recruitment of ER is unknown. However α dystroglycan is a potential regulator of postsynaptic ER recruitment. α Dystroglycan forms a complex with synaptopodin, via MAGI-1 (Patrie et al 2002), and synaptopodin is the only known protein required for SA recruitment. α Dystroglycan is expressed at the NMJ, purkinje cell, and the mossyfiber synapses (Satz et al 2010), where ER is heavily recruited in the postsynapse. Because of its interaction with synaptopodin, and location of expression, it is possible that α dystroglycan plays a role in ER recruitment in an analogous way to NCAM recruiting TGN.

The postsynaptic recruitment of ER, and the potential targeted exocytosis of receptor, would be a form of synaptic oriented polarization. Often in polarized cells, surface proteins undergo transcytosis. The classic model for neuronal transyctosis is NgCAM, which first exocytoses at the somatodendritic membrane, endocytoses, transports, and then exocytoses, for the second time at the axon (Wisco et al 2003). Interestingly, NMDAR-SAP102 transport packets recycle back and forth between an endosome and the surface membrane before reaching the synapse (Washbourne et al 2002). Hence, intracellular trafficking to the synapse is often convoluted, and can involve indirect trafficking or transcytosis. Whether there is a relationship between synaptic organelle polarization, transcytosis, and receptor insertion is not known.

It is possible that ER plays a role in receptor-scaffold interaction. Jeyifous et al found that NMDAR packaged with SAP97 and CASK in the ER. Interestingly, the ER secretory pathway for NMDAR-SAP97 packages was atypical. Packages transported in a specialized ER that merged directly with dendritic golgi outposts. Whether spine ER, SA, or t-tubules can package receptors, and whether this is inducible rather than constitutive, is unknown.

In summary, little is known about the postsynaptic recruitment and function of ER or its derivatives. However ER at the synapse is correlated with synaptic strength.

How ER derived t-tubules are recruited to the postsynapse, and their role in packaging, receptor mobility, and synaptic strengthening is examined in this thesis.

Agrin induced AChR clustering.

Agrin induced AChR clustering in vitro is a good model to investigate postsynaptic diffusion versus insertion because, as discussed above, diffusion-trapping is well established and there is evidence for direct insertion. Below I will introduce agrin induced clustering, and highlight its advantages for this study.

The initial data for the diffusion-trap model came from AChR clustering, over 35 years ago (Axelrod et al 1976). The addition of the z-splice variant of agrin to muscles in vitro is sufficient to induce AChR clustering (reviewed in McMahan 1990). In vivo, this form of agrin is secreted by the motor neuron; is sufficient to cluster AChRs in vivo; and is necessary for normal NMJ formation and development (reviewed in Ruegg et al 1992). Experimentally, AChRs can be labeled with bungarotoxin (BTX) without inhibiting agrin-induced clustering. Therefore AChR clustering is amenable to live cell imaging of pulse-chased AChR-BTX conjugated to a fluorophore, or BTX-biotin-streptavidin QDT for single molecule imaging.

The agrin signal is transduced by multiple receptors. Muscle specific kinase (Musk), is a transmembrane tyrosine kinase that phosphorylates AChR after agrin binding, and is required for AChR clustering in vitro (Glass et al 1996) and NMJ formation in vivo (DeChiara et al 1996). The adhesion molecules α dystroglycan has also been proposed as a receptor (Gee et al 1994). α Dystroglycan knockout is embryonic lethal, but chaemeric mice survive and have misformed NMJs (Cote et al 1999). Furthermore α dystroglycan knockdown in myotubes allows cluster formation, but the clusters are large and weak (not AChR dense)(Jacobson et al 2001). Most recently "low density lipoprotein receptor related protein 4" (Lrp4) was found to be a co-receptor with Musk, and required for normal NMJ formation (Kim et al 2008).

Why there might be so many agrin receptors, and if they might have different functions is not known.

The agrin signaling cascade starts with Musk and its co-receptor Lrp4 binding agrin, followed by a series of self and other phosphorylations including the Src family kinases (Src) (reviewed in Wu et al 2010). Most notably, AChR phosphorylation by Musk and Src increases the affinity of AChR for an additional rapsyn (Moransard et al 2003). This leads to a ratio of 2 rapsyns per AChR within 40 minutes after agrin, and this addition is thought to happen in surface (non-t-tubule) caveolin-3 lipid rafts (Zhu et al 2006). Furthermore, rapsyn is able to bind to the cytoskeleton and α dystroglycan in order to anchor the AChR in the postsynapse (Cartaud et al 1998). Hence AChR interacting with two rapsyns is the state of assembly at a mature cluster.

AChR clusters form and mature in at least three steps in vitro (Bruneau et al 2005). Before agrin is added, 'seed' clusters are present. These clusters are very weak, and contain a relatively very low density of AChR. Shortly after agrin, clusters form at 'seed' cluster sites. These weak clusters are visible within an hour, and are thought to be Rac and RhoA dependent (Weston et al 2003). Several hours later clusters become stronger and increase their density of AChRs. The fast induction by agrin and combined with the stereotyped cluster maturation (from formation, to weak, to strong clusters) facilitates the study of clustering at precise stages. Furthermore it is clear that AChR density can be used to follow the stage or strength of the cluster.

It is certain that agrin induces cluster formation in vitro, but it's precise role in vivo is perhaps more complicated (reviewed in Kummer et al 2005). Before the motor neuron arrives in vivo, small agrin-independent AChRs clusters already exist and are called the 'prepattern'. Furhtermore AChR clusters dissipitate in the presence of acetylcholine, but this is inhibited in the presence of agrin. Hence agrin is

considered an anti-declustering agent, counteracting the loss of stability (declustering) induced by acetylcholine and activity.

In summary of the introduction, the first main question to address is whether receptors insert immobile in the postsynapse, as apposed to diffusing in and then becoming immobile. Secondly, there is a correlation between specific states of receptor-scaffold complex assembly and receptor mobility, but where the assembly happens is unknown. The immobile assembly state is assumed to happen at the synapse, after receptors diffuse in, but if receptors insert immobile then they might be preassembled with scaffold (in the immobile configuration) before insertion so that they are prepared for immobility. Thirdly, if receptors are packaged in vesicles before insertion then there must be an intracellular packaging and trafficking organelle of unknown identity. Finally, there must also be a mechanism to recruit the packaging organelle and target immobile packages for immobile insertion. These questions are primarily addressed by tracking AChR trafficking to clusters after the addition of agrin to C2C12 myotubes in vitro.

Results.

1. AChRs diffuse into weak clusters, but not into strong clusters.

Do AChRs diffuse or insert into clusters after agrin? We first investigated AChR diffusion by measuring fluorescence recovery after photobleaching (FRAP) at clusters, using a fluorescently tagged bungarotoxin (BTX-488) to label AChRs. Before agrin, 'seed' clusters (Bruneau et al 2005) had a large FRAP within 7mn, suggesting diffusion mediated recovery (68% FRAP average, $p< 0.01$) (fig 1a). After 45mns agrin, weak AChR clusters formed, which had low density AChR signal and a more modest FRAP (53% FRAP, $p< 0.01$) than seed clusters (fig 1a). After three hours agrin or more, weak clusters strengthened by increasing their AChR density but surprisingly there was little or no FRAP at strong clusters, suggesting little or no diffusion (7% FRAP, $p< 0.01$, 3hrs agrin) (fig 1a). 'Weak' and 'strong' clusters were further defined by quantifying their respective low and high AChR and rapsyn densities from fluorescent signal intensities. Weak clusters at 45mn were distinguishable from strong clusters at 3hrs by their AChR and rapsyn densities ($p<0.0001$) (fig 1b). The difference in AChR trafficking and postsynaptic assembly at weak versus strong clusters will be the focus of this investigation.

The fast FRAP (within 7mn) at weak clusters suggests a fast AChR diffusion, whereas little or no FRAP (within 7mn) at stronger clusters suggests little or no diffusion and a high immobile fraction (Sprague and McNally 2005). To confirm these suggestions we tracked single AChR molecules at weak and strong clusters, using quantum dots (QDT)(Triller and Choquet 2008). Consistent with the FRAP data (fig 1a), we observed a trend of restricted AChR-QDT diffusion within weak clusters before 45mn agrin, but immobility at strong clusters after 3hrs agrin ($p=0.0084$, comparing the diffusion coefficients at 45mn and 3hrs clusters) (fig 1c) (supp movies 1 and 2). We frequently observed AChR-QDTs diffusing from outside to inside weak clusters, but surprisingly, we rarely saw diffusion into strong clusters (fig 1c, far right graph). We confirmed this surprising observation by imaging AChR-

QDTs around strong clusters over longer periods of time (20mn, 1Hz) (supp movie 3).

Together, the FRAP and QDT data demonstrate that AChRs diffuse into weak but not strong clusters (fig 1d). This raises the following question: If AChRs do not diffuse into strong clusters, then how do they traffic there?

Figure 1.

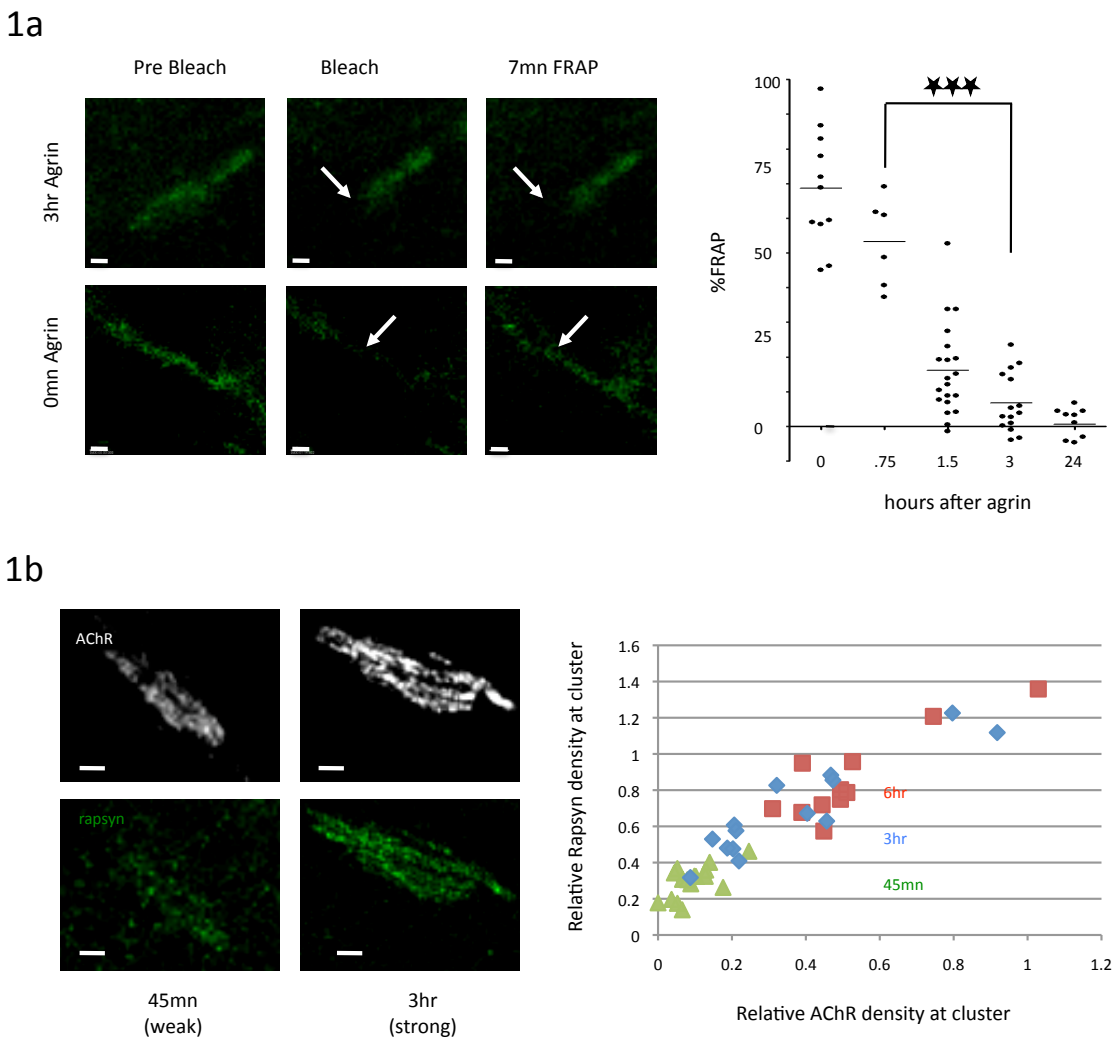

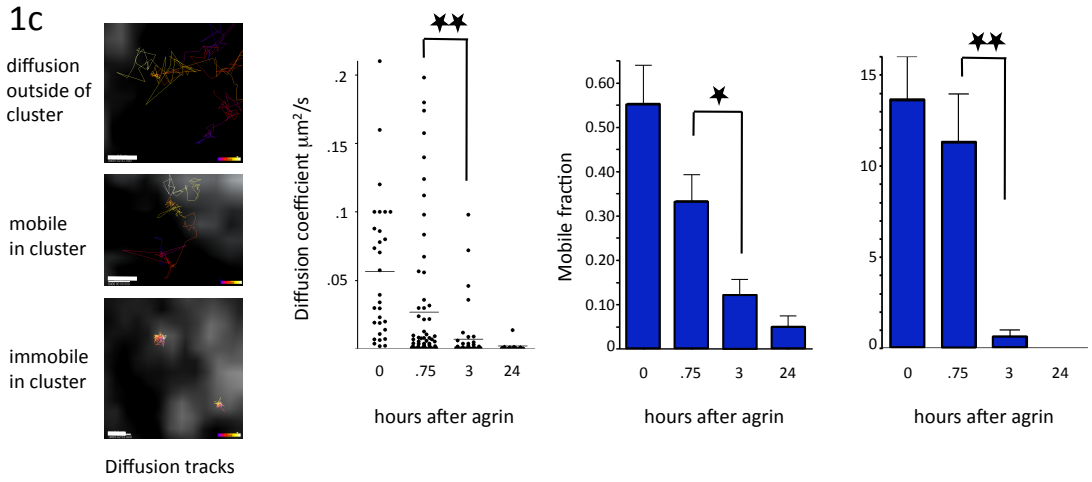

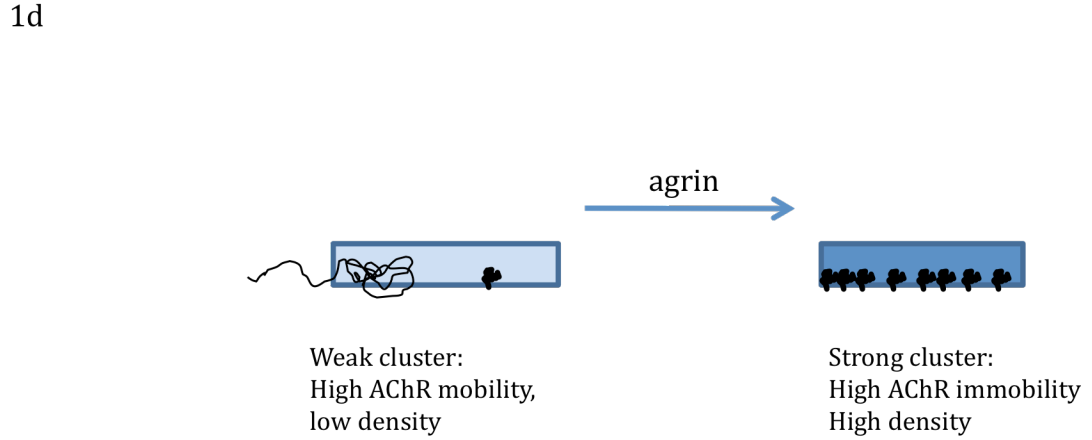

Figure 1. Receptors diffuse into weak clusters but not strong, and receptors are immobile at strong clusters.

1a. Left: representative images of 7mn FRAP at strong (3hr agrin, top row), and weak (0mn agrin, bottom row), AChR (green) clusters; blue rectangles mark target for bleaching; scale bars are 2µm. Right: quantification of percent FRAP at clusters after different times agrin; ANOVA p< 0.0001, (t-test between 0.75 and 3hrs, p<0.0001) .

1b. Left: representative images of rapsyn (green) and AChr (white) staining at weak (45mn, left column) and strong (3hr, right column) clusters; scale bar is 1.5µm. Right: quantification of rapsyn and AChR signal densities at 45 (green), 3hr (blue), and 6hr (red) clusters.

1c. Left: representative images of AChR-QDT tracks showing free diffusion outside of a cluster (top), restricted diffusion within a cluster (middle), and immobility in a cluster (bottom); scale bar is 0.2µm. Moving from left to right, the first graph quantifies the diffusion coefficients from tracks inside cluster (t-test between 0.75 and 3hrs, p=0.002); the second graph quantifies the percent of mobile AChR-QDTS in the cluster(t-test between 0.75 and 3hrs, p=0.017); and finally the number of AChR-QDTs observed moving into the cluster(t-test between 0.75 and 3hrs, p=0.004), all after agrin. ANOVA p< 0.0001 for all three graphs.

1d. Summary of figure 1 findings. Left, weak clusters have less receptors (indicated by the lighter shade of blue in the rectangle representing the cluster), and receptors can diffuse into and inside the cluster (the black lines represent diffusion tracks). Right, there is a higher density of receptor at strong clusters, and receptors are immobile.

2. Direct insertion of immobile AChRs drives the increase in AChR number at strengthening clusters.

If AChRs do not diffuse into strong clusters, they are most likely inserted. Consistent with insertion, we noticed a slow FRAP (45-90mn) at clusters, which was sensitive to the insertion blocking drug n-ethylmalemide (NEM) (fig 2a). Surface AChRs are labeled in the FRAP experiments, therefore this slow, NEM sensitive FRAP at strong clusters is mediated by a surface AChR pool. This implies insertion of AChRs that trafficked from the surface to the cluster.

Taking advantage of this surface to cluster trafficking, we pulse-chased surface labeled AChR-QDTs to see how individual molecules insert at clusters. Imaging strong clusters, with the optical focus on the bottom of the cell, we saw QDT-AChRs suddenly appear in the middle of clusters (fig 2b), which is consistent with insertion. Furthermore, we did not see diffusion after AChR-QDT insertion, only immobility (fig 2b, arrows). Imaging clusters on the side of a cell, we saw QDT-AChR transported in long straight lines (indicative of microtubule transport) towards clusters (supplemental fig 1), before arriving immobile in the cluster. This single molecule study of insertion shows that surface labeled AChRs are inserted directly into strong clusters, where they are immobile within a second, or perhaps immediately.

To compare the contribution of surface versus inserted AChRs to strengthening clusters, we used a simultaneous surface and insertion assay on live cells. We added agrin for two hours, labeled surface AChR with BTX-488 to saturation, washed, and then left BTX-555 in the bath for 40mn to label newly inserted receptors. Comparing the difference between surface and inserted labels, it was clear that the inserted label dramatically increased at strong clusters, while the surface label did not (fig 2c). Therefore the addition of AChR to strengthening clusters is driven by insertion.

The same protocol at different times after agrin, followed by fixation, revealed greater insertion at strong clusters (1.5 and 8hrs after agrin), than weak (before 45mn) (fig 2c). Interestingly, 24hrs after agrin, the difference between surface and inserted labels was similar to that of weak clusters, implying a return to diffusion or a different mechanism of AChR addition. The time course of increased insertion at the cluster (1.5-8hrs agrin, fig 2c), paralleled the time course of increased rapsyn, or strengthening, at the cluster (fig 1b).To directly correlate insertion with strength, we measured AChR insertion as well as rapsyn density at clusters. We measured insertion and rapsyn after 2hrs agrin, when there is most heterogeneity in cluster strength: some are strong, others weak. Plotting rapsyn versus inserted AChR density, we found a positive correlation ($r= 0.87$) between strength and insertion after 2hrs agrin. Therefore insertion not only adds the majority of AChRs to strengthening clusters, it also correlates with cluster strength. Furthermore, even when cells were exposed to agrin for the same time (2hrs), some clusters had more insertion and rapsyn than others, suggesting insertion is a stronger driving force for cluster strength than time after agrin alone.

Using FRAP and single molecule tracking, we have shown that surface labeled AChRs insert directly into clusters as immobile units. Surface to cluster AChR trafficking drives receptor addition to strengthening clusters, and correlates with strengthening. This raises two questions. How do AChRs traffic from surface to cluster, and why does this trafficking correlate with cluster strengthening?

Figure 2.

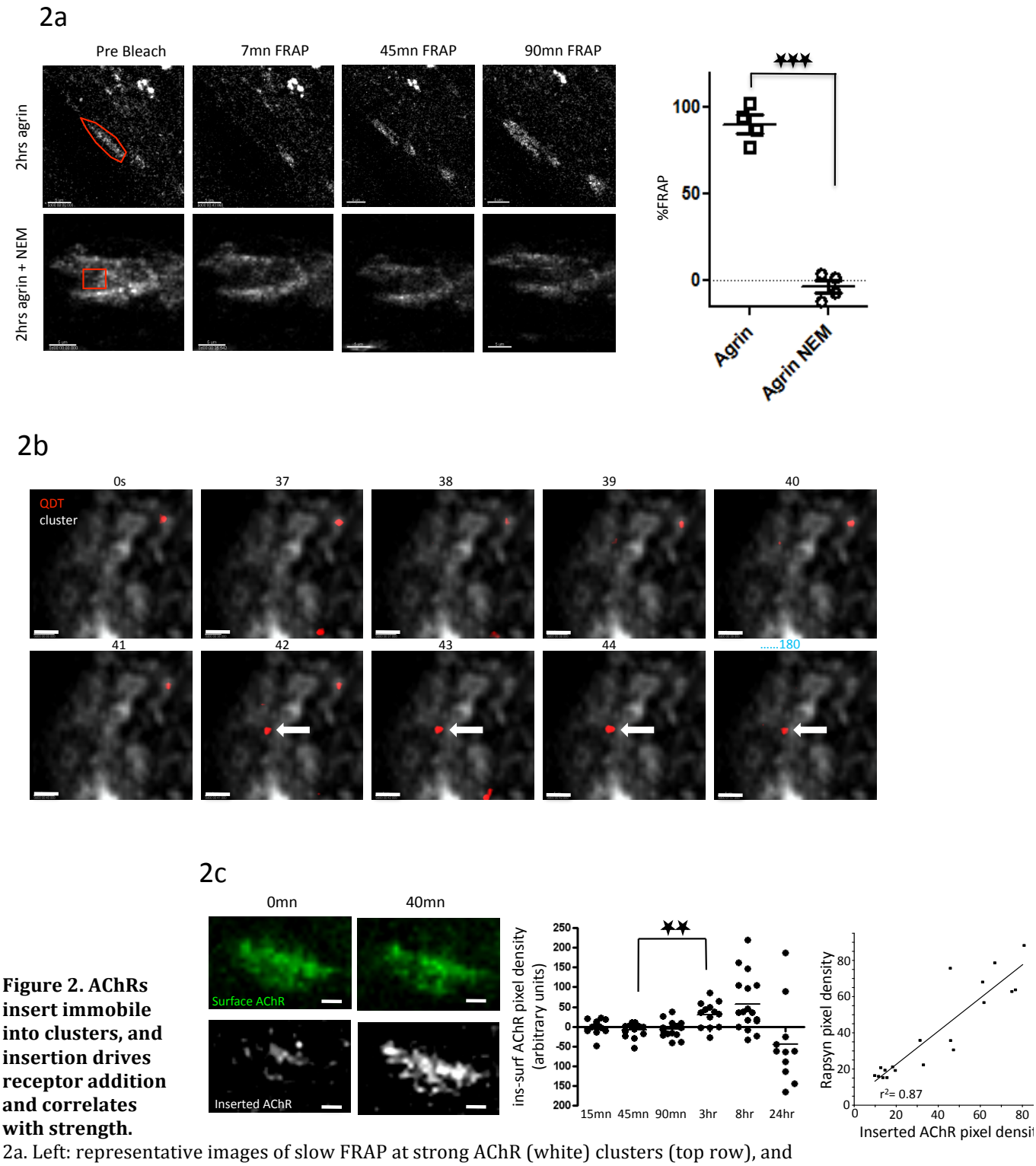

Figure 2. AChRs insert immobile into clusters, and insertion drives receptor addition and correlates with strength.

2a. Left: representative images of slow FRAP at strong AChR (white) clusters (top row), and inhibition of slow frap with NEM (bottom row); red boundaries mark bleaching targets; scale bar is 5µm. Right: quantification of slow FRAP after 45mn at control (DMEM treated) versus NEM treated cells. T-test p=0.001.

2b. AChR clusters (white) on the bottom of the cell were imaged every 1s. After 37s an AChR-QDT (red spot) appears immobile (white arrow); scale bar is 5μm.
2c. Left: Surface (green) versus inserted (white) AChR label 40mn time-lapse at 2hrs agrin clusters; scale bar is 2.5μm. Graphs moving left to right: quantification of the difference in inserted and surface labels pixel densities at clusters at different times after agrin (3hrs vs. 45mn t-test, p=-.0061); qunatification of the correlation (r2=0.87) between inserted AChR (x-axis) and rapsyn intensities at 2hr agrin clusters.

3. After agrin surface AChRs endocytose and traffic via caveolin-3 t-tubules, and t-tubules are recuited to clusters.

How do surface AChRs traffic to clusters? In the FRAP and QDT experiments we saw that pulse-chased, surface labeled AChRs insert at clusters, which suggests that AChRs traffic form the surface to the cluster via an intracellular compartment. Therefore we performed 4D imaging (time-lapse in x-y and z) of pulse-chased AChR-BTX-488, expecting to see an intracellular accumulation of AChR. We defined 'intracellular' as being inside the peripheral border of the cell, which was defined in x,y, and z. Before the addition of agrin, AChR was predominantly at the surface membrane, and 'seed' clusters were visible (fig 3a). Between 45mn and 3hrs agrin, intracellular AChR accumulations were often larger and brighter than clusters; a loss of membrane AChR was visible; and seed clusters converted to weak clusters (fig 3a). After 3hrs, the intracellular AChR accumulation often decreased in size but not brightness, while weak clusters became strong. Fixing and staining for rapsyn after 4D imaging, we found stronger clusters nearby intracellular accumulations and weaker clusters further away; even when clusters were in the same cell (supplemental fig 2). Together, this 4D imaging revealed a dramatic intracellular AChR accumulation after agrin. Furthermore, this intracellular accumulation often formed faster, larger, and brighter than surface clusters, and the proximity of the cluster to the accumulation seemed to correlate with cluster strength.

To identify which intracellular compartments accumulated AChRs, we fixed cells after 45mn agrin, the peak of intracellular accumulation, and then performed an immunocytochemical screen with antibodies against intracellular organelle markers. We screened with antibodies against the Rab family (Rab4,5,6,7,9,11,27)

and t-tubule proteins (dysferlin, caveolin-3, and myotubularin (MTM1)) because Rabs are classical markers of endosomal trafficking, and t-tubules are a muscle specific trafficking system (Stein et al 2003 and Al-Qusairi and Laporte 2011). We found strong AChR colocalization with the t-tubule marker caveolin-3 (fig 3b), weak colocalization with t-tubule markers dysferlin and MTM1, but little colocalization with the Rab family. Furthermore intracellular accumulations after agrin did not colocalize with degradation pathway markers LAMP1 and LBPA (supplemental fig 3). Therefore caveolin-3 and the t-tubule organelle are candidates for surface-to-cluster AChR trafficking after agrin.

To more accurately trace the trafficking pathway form surface to cluster, we pulse-chased QDT-AChR after agrin, fixed at different times, and stained for t-tubule markers. This QDT-AChR pulse chase has the advantage that, unlike BTX-488 pulse-chase or fixation after agrin, the QDT label does not penetrate surface accessible endosomes, and starts specifically at the peripheral surface plasma membrane (supplemental fig 4). We found that pulse-chased AChR-QDTs have a sharp early (15mn agrin) peak of colocalization with dysferlin, a broad intermediate (45mn) peak with caveolin-3, and a persistent late (3hr) peak with myotubularin (MTM1) (fig 3c and supplemental fig 4). We also found that 70% of AChR-QDTs endocytose with bath rhodamine dextran during the first 15mn after agrin (fig 3c). Therefore AChR-QDTs endocytose from the plasma membrane and traffic via the t-tubule system after agrin.

While looking at caveolin-3 images we noticed that caveolin-3 often invaded the space around strong clusters (fig 3d). We quantified the volume of caveolin-3 fluorescent signal within 3um of the cluster, and found that strong clusters recruited caveolin-3, but weak clusters did not ($p=0.003$, fig 3d). Furthermore, 2hrs agrin clusters have heterogeneous strength: some are weak, others strong. Performing the same insertion and fixation assay as before (fig 2c), we stained with caveolin-3 and found a positive correlation ($r^2=0.81$) with insertion: the more caveolin-3 recruited to the cluster, the more insertion.

Hence, after agrin, AChRs traffic through the caveolin-3 and t-tubule system, and the t-tubule organelle remodels, and is recruited to the cluster. Furthermore there is a correlation between the caveolin-3 t-tubules recruitment and AChR insertion at the cluster. This begs the question of whether caveolin-3 and t-tubule trafficking are required for AChR insertion and cluster strengthening.

Figure 3.

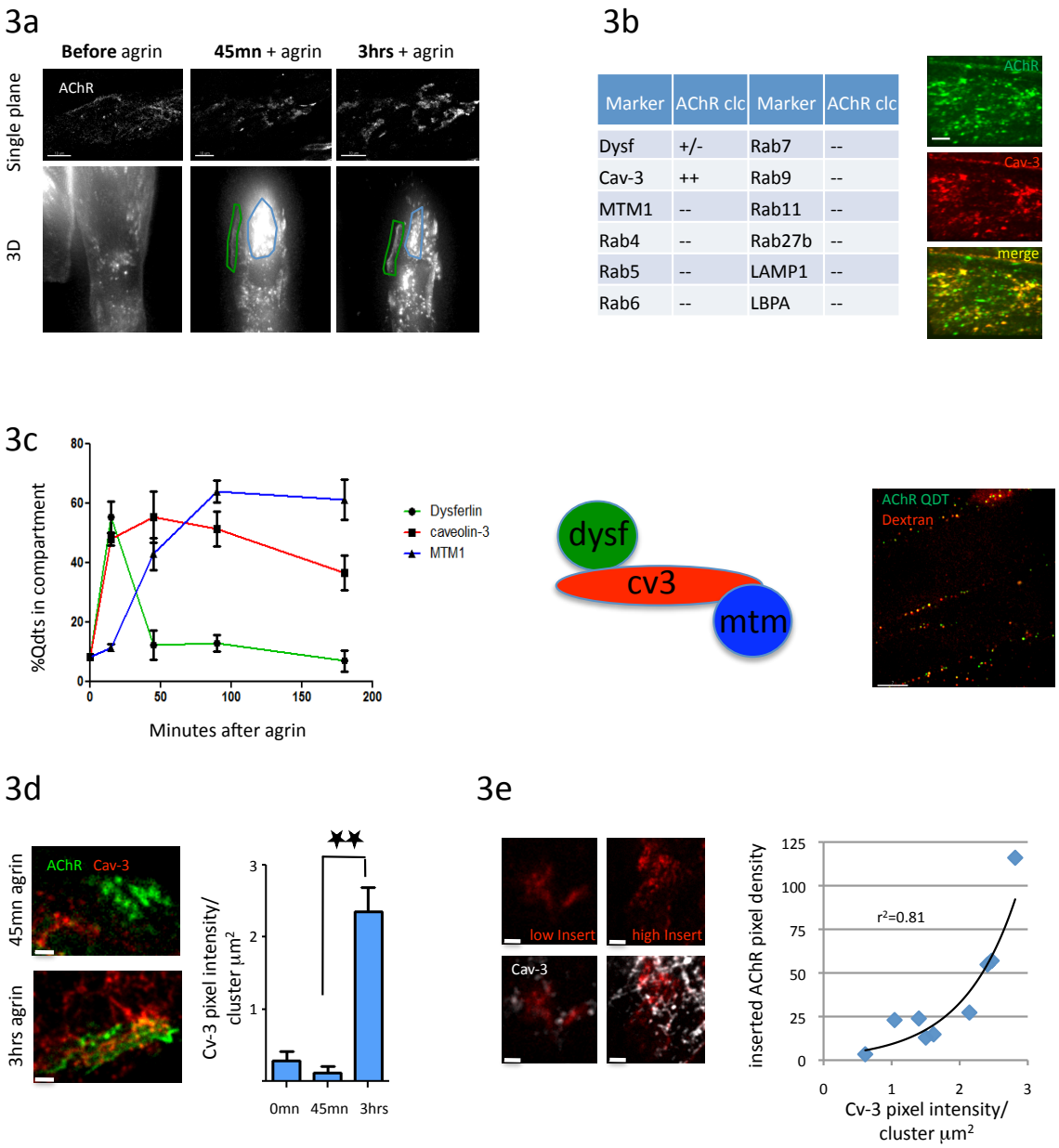

Figure 3. AChRs accumulate in and traffic through t-tubules after agrin; and t-tubules are recruited to strong clusters.
3a. 4D timelapse analysis of surface AChR after agrin. Single planes (top row) of clusters before agrin, and 45mn and 3hrs after; 3D reconstructions below; green borders mark a forming cluster and the blue surrounds an intracellular accumulation; scale bars are 10μm.
3b. Left: table of screened compartments that colocalize with intracellular AChR accumulations after agrin (++=strong colocalization, +/-= mild colocalization, and --= little or no colocalization). Right: representative image of AChR (green) and caveolin-3 (red) staining after 45mn agrin; scale bar is 3μm.
3c. Left: quantification of percentage of pulse-chased AChR-QDTs colocalizing with t-tubule compartments (dysferlin (green line), caveolin-3 (red line), and myotubularin (MTM1)(blue line). Middle, schematic of t-tubule early (dysf = dysferlin, green), intermediate (cv3= caveolin-3, red), and late (mtm = MTM1, blue) trafficking compartments. Right, single confocal plane image of AChR-QDT colocalizing with rhodamine dextran (red) 15mn after agrin; scale bar is 7μm.
3d. Left: representative single confocal plane images of caveolin-3(red) and AChR (green) at weak (45mn agrin, top) and strong (3hr agrin, bottom) clusters; scale bar is 2μm. Right: quantification of caveolin-3 signal intensity at the cluster, divided by the area of the cluster (henceforth referred to as caveolin-3 'recruitment'); t-test between 3hrs and 45mn agrin, p=0.003.
3e. Left: representative images of inserted AChR (red) and caveolin-3 (white) after 2hrs agrin; example of little insertion (left column), and high insertion (right column); scale bars are 2μm. Right: quantification of correlation (r^2=0.81, non-linear fit) between recruited caveolin-3 and inserted AChR at clusters, after 2hrs agrin.

4. t-tubules, and caveolin-3 trafficking, are required for AChR insertion and cluster strengthening, and recruitment of t-tubules to clusters correlates with cluster strength.

To test the requirement of t-tubules for AChR insertion and cluster strengthening we detubulated cells, which acutely and reversibly incapacitates t-tubules by osmotic shock (Al-Qusairi and Laporte 2011). Detubulated cells formed clusters, and non-cluster AChR diffusion was unaffected by detubulation (supplemental fig 5). However, clusters in detubulated cells did not strengthen. 3hr clusters in detubulated cells had similar AChR and rapsyn densities to 45mn clusters in normal cells (fig 4a). Normally after 3hrs agrin, nearly all AChRs are immobile in clusters (fig 1c), whereas in detubulated cells the AChR-QDT mobile fraction was similar to 45mn agrin clusters in normal cells (4a). Furthermore, caveolin-3 recruitment and AChR insertion at clusters was strongly reduced in detubulated cells (fig 4b, blue squares) compared to control (fig 4b, red squares). In summary, clusters form but

do not strengthen, and there is little caveolin-3 and AChR insertion at clusters in detubulated cells.

It was recently shown that LRP4 is a co-receptor for agrin (Kim et al 2008). Because LRPs are trafficking molecules, we investigated the effect of LRP4 inhibition on AChR trafficking. Before adding agrin, we pretreated cells with the LRP4 ligand APOE4, to see how caveolin-3 t-tubule trafficking is affected. In APOE4 treated cells, AChRs were immediately trafficked to MTM1, and not caveolin-3 (fig 4c), validating APOE4 as a tool to inhibit agrin-induced caveolin-3 trafficking. In APOE4 treated cells, clusters formed but did not increase their rapsyn and AChR densities to strong levels, and AChRs were mobile in the clusters after 3hrs agrin (fig 4d). Hence LRP4 inhibition prevents agrin-induced caveolin-3 trafficking, and inhibits cluster strengthening, but not formation.

In summary, detubulation and APOE4 treatment show that t-tubule and caveolin-3 trafficking are required for cluster strengthening and AChR insertion. This still leaves two questions open. How do receptors traffic from t-tubules to clusters, and why is t-tubule trafficking required strengthening?

Figure 4.

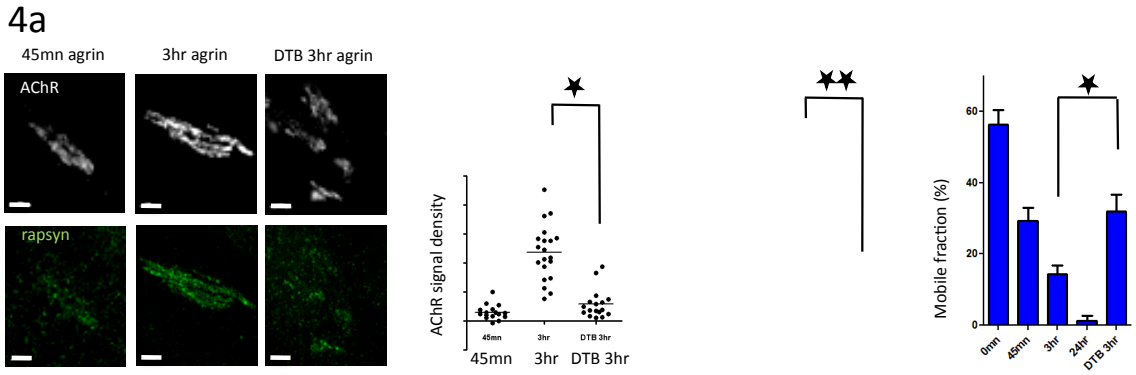

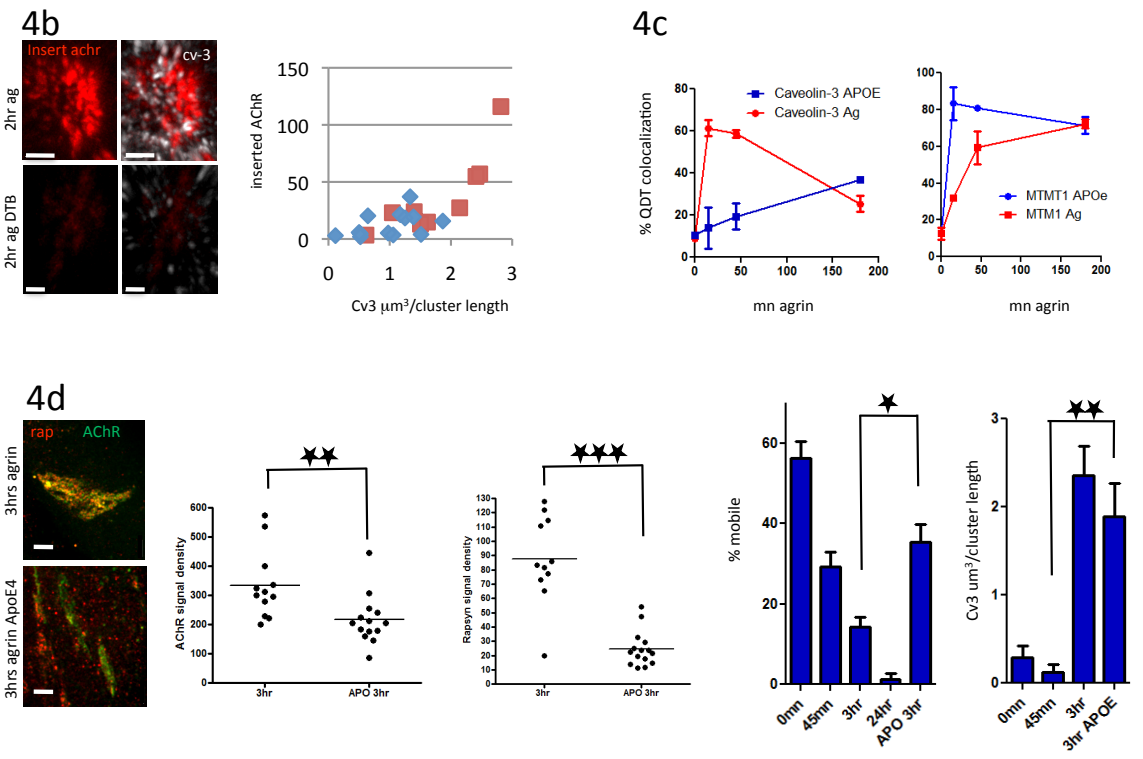

Figure 4. T-tubules and caveolin-3 trafficking are required for cluster strengthening.
4a. Left: representative images of AChR (white) and rapsyn (green) clusters after 45mn and 3hrs agrin, and after detubulation (DTB) followed by 3hrs agrin; scale bars are 1.5µm. Right: moving left to right, quantification for AChR (p=0.024) and then rapsyn (p=0.0066) signal densities at clusters; and quantification of the mobile fraction from AChR-QDT data (3hrs agrin in control versus detubulated cells, p= 0.015).
4b. Left: representative images of inserted AChR (red) and caveolin-3 (white) after 2hrs agrin in control (top) and detubulated (bottom) cells; scale bars are 2µm. Right: quantification of inserted AChR and recruited caveolin-3 at clusters in control cells (red, and fig 3d) and detubulated cells (blue).
4c. Quantification of percent pulse-chased AChR-QDT colocalization with caveolin-3 (left) and MTM1 (right) at different times after agrin in control cells (red lines) versus APOE4 treated cells (blue lines). APOE4 is an LRP4 ligand, and LRP4 signaling is required for clustering. This figure shows that ApoE4 is a tool to disrupt caveolin-3 trafficking after agrin.
4d. Left: representative images of AChR and rapsyn staining at clusters in control (top)cells and APOE4 (bottom) treated cells after 3hrs agrin; scale bars are 1.5µm. Right: moving left to right, quantifications of AChR (t-test, p=0.0065) and then rapsyn(t-test, p<0.0001) densities at clusters in control and APOE4 treated cells; followed by quantification of the immobile fraction (p=0.0351) from AChR-QDT data; and then caveolin-3 recruitment after APOE4 treatment (control versus APOE4 treated cells after 3hrs agrin, p=0.003).

5. AChRs preassemble with rapsyn inside the cell before myosinVa dependant insertion at the cluster.

How might AChRs traffic from t-tubules, and insert at clusters? The MyosinVa/Rb27a complex has been implicated in AChR exocytosis at NMJs (Roeder et al 2008). We found that pulse-chased AChR-QDTs colocalized with the exocytic marker Rb27a within three micrometers of clusters after 45mn and 3hr chase but not throughout the cells in general (fig 5a). We also obtained images of AChR-QDTs costained with Rb27a vesicles apparently docked on clusters (fig 5a). Furthermore Rb27a vesicles were spatially organized around cav-3 t-tubules, and often appeared in contact with tubules (fig 5a, furthest right image). This suggests that AChRs exocytose at the cluster in Rb27a vesicles.

MyosinVa forms a complex with Rb27a, and MyosinVa knockdown has been shown to block AChR exocytosis at NMJs in vivo (Roeder et al 2008). Because AChRs colocalize with Rb27a, and because MyosinVa knockdown is known to block AChR insertion in vivo, knocking down MyosinVa with siRNA should block AChR insertion at clusters, but allow t-tubule AChR trafficking. We transfected day 3 myotubes with lentiviral transduction particles against myosinVa, and measured knockdown by immunostaining for myosinVA on day 6 (supplemental fig 6). In knockdown and adjacent control cells, AChRs trafficked through caveolin-3 t-tubules after agrin. As predicted from a myosinVa insertion block, AChRs accumulated inside knockdown cells and insertion was inhibited at strengthening clusters (2hrs agrin). Notably, intracellular accumulations were much larger and brighter than clusters in knockdown and control cells (supplemental fig 7). Furthermore, clusters did not strengthen and increase their rapsyn densities, nor did AChRs shift towards immobility in 3hr clusters (fig 5b).

Intracellular AChR accumulations in control cells (fig 3a), and particularly in myosinVa knockdowns (supplemental fig 7), were often larger and more AChR dense than clusters. This suggests that AChR, and perhaps rapsyn, densities at the

cluster, might be predetermined inside the cell before cluster insertion. In other words, cluster strengthening might happen inside the cell, and not at the cluster.

Because increased rapsyn density is a marker for strengthening, and because rapsyn increases its association with AChR after agrin (Moransard et al 2003), we tested intracellular strengthening by staining intracellular AChR accumulations for rapsyn after agrin, and after pulse-chasing AChR-QDTs. Intracellular AChR accumulations colocalized well with rapsyn after agrin (5c). Furthermore, pulse-chased AChR-QDTs gradually increased their colocalization with rapsyn, even when they were inside the cell and not yet inserted at the cluster (fig 5c). Pulse-chased AChR-QDTs also increased their colocalization with rapsyn after 3hrs agrin, but not after 24 hours agrin or without agrin (supplemental fig 8). We also found stronger colocalization of rapsyn with MTM1, and Rb27a vesicles near clusters, compared to dysferlin and membrane AChR (supplemental fig 9). Together this suggests that AChRs preassemble with rapsyns, in an AChR-rapsyn transport package, inside the cell before arriving at the cluster. Therefore cluster strength is determined intracellularly and not at the cluster.

If AChRs are pre-packaged with rapsyn before insertion at clusters, then blocking exocytosis with myosinVa knockdown should allow strengthening inside the cell, but not at the cluster. In myosinVa knockdown cells, pulse-chased AChR-QDTs increased their colocalization with rapsyn inside the cell (fig 5c), but clusters did not strengthen rapsyn densites (fig 5b, and summarized in 5d). When cells were treated with APOE4, to prevent caveolin-3 trafficking, pulse-chased AChR-QDTS did not increase their colocalization with rapsyn inside the cell (fig 5c), nor at the cluster (fig 4d).

In summary the strengthening process of clusters occurs intracellularly, not at the cluster. AChRs pre-package with rapsyn inside the cell before inserting at the cluster, and APOE4 treatment shows that caveolin-3 trafficking is required for this prepacking. Finally, intracellular AChR-rapsyn packaging and insertion are required

for cluster strengthening, because if exocytosis in blocked (myosinVA knockdown) strengthening still occurs intracellularly, but not at the cluster.

Figure 5.

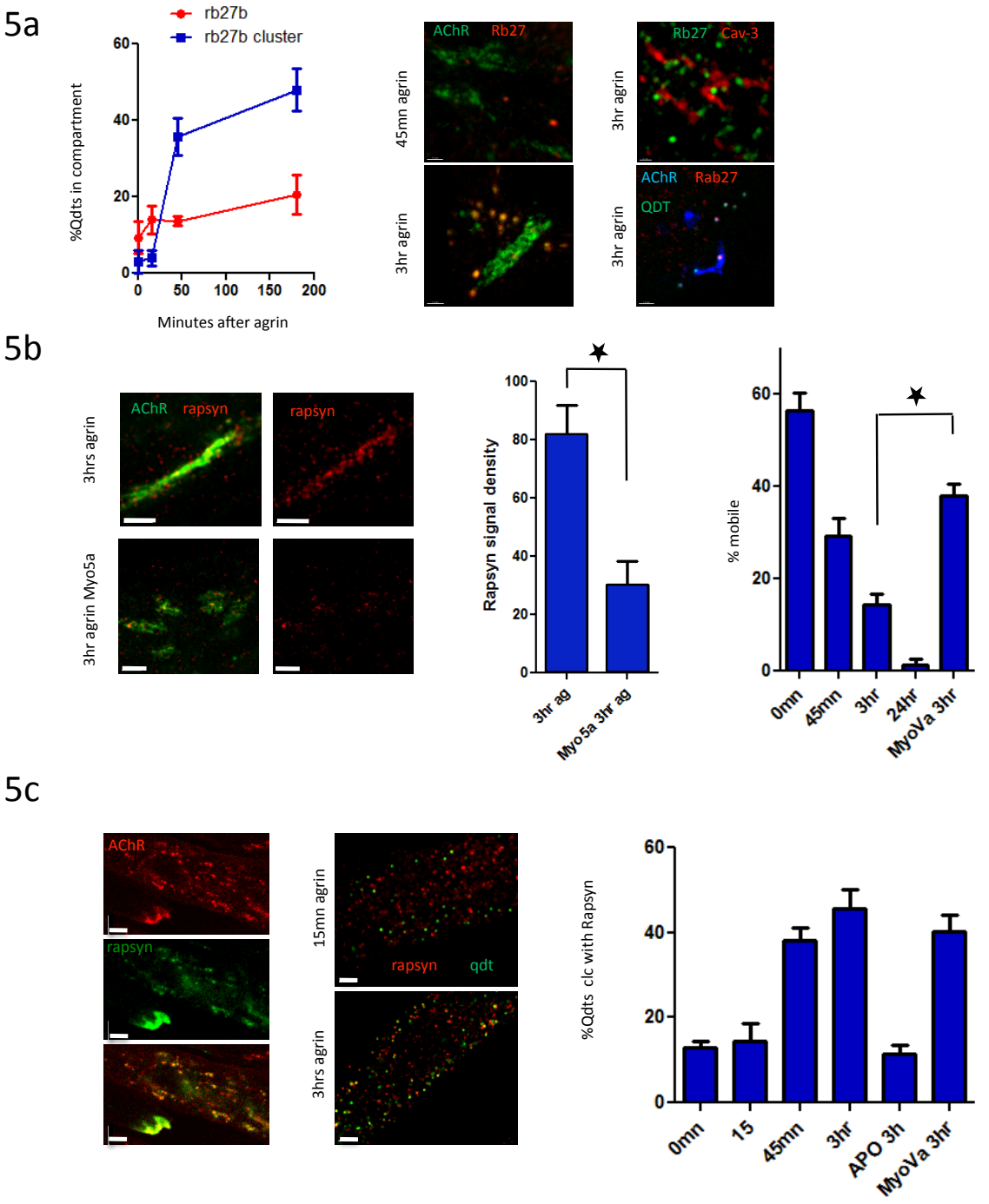

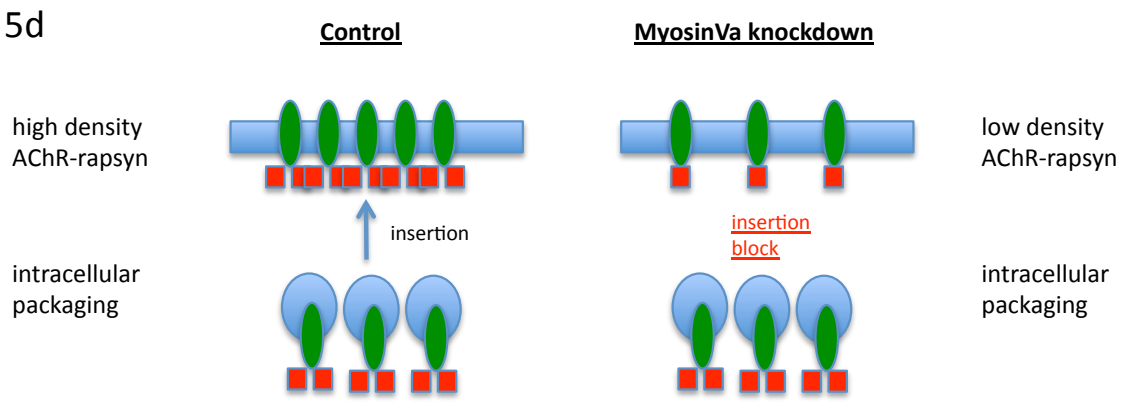

Figure 5. MyosinVa dependent AChR insertion is required for AChR-rapsyn packaging at the cluster but not intracellularly.
5a. Left: quantification of pulse-chased AChR-QDT with Rb27b throughout the cell (red) and within 3μm of the cluster (blue). Right: moving left to right, image of pulse-chased AChR-BTX488 recruited to Rb27a vesicles after 45mn (top) and 3hr agrin (bottom) (scale bar is 1.5μm); image of Rb27a and caveolin-3 staining (top)(scale bar is 0.5μm); image of AChR cluster (blue), AChR-QDT (green), and Rab27b (red) (scale bar is 1.5μm) (bottom);.
5b. Left: AChR and rapsyn staining at clusters after 3hrs agrin in control and myosinVa knockdown cells; scale bars are 3μm. Right: quantification of rapsyn at clusters in control and myosinVa knockdown cells (t-test p=0.0351), and quantification of mobile fraction from AChR-QDT data (3hr agrin control versus myosinVa t-test, p= 0.035).
5c. Left: in the first column of images, AChR and rapsyn colocalize throughout the cell after 3hrs agrin; in the next column of images, pulse-chased AChR-QDT colocalization with rapsyn after 15mn and 3hrs agrin; scale bars are 5μm. Right: quantification of pulse-chased AChR-QDT at different times after agrin, in APOE4 treated cells, and myosinVa knockdown cells (3hrs agrin in untreated versus APOE4 treated cells t-test, p=0.027).
5d. Summary schematic of intracellular strengthening. The results show that rapsyn is prepackaged with AChR inside the cell and not at the cluster, because blocking insertion allows an increase in intracellular AChR-rapsyn packaging, but inhibits AChR-rapsyn packaging at the cluster. Left is a control cell, demonstrating high density AChR (green) packaged with 2 rapsyn (red) at clusters (blue rectangle). AChR-2x(rapsyn) packages insert at clusters. Right, when insertion is blocked (red writing), AChR-2x(rapsyn) packaging occurs inside the cell, but not at the cluster.

6. α Dystroglycan is not prepackaged with AChR, but recruits caveolin-3 t-tubules.

Having shown that rapsyn is prepackaged with AChR intracellularly, we wanted to know if other molecules in the postsynaptic assembly are similarly pre-packaged. Staining for molecules that colocalize with AChR inside the cell after agrin, we found that the scaffold molecule utrophin was pre-packaged with AChR, but the laminin binding protein α dystroglycan was not. Furthermore pulse-chased AChR-QDT increased colocalization with utrophin, but decreased with α dystroglycan (fig 6a).

This implied that α dystroglycan traffics to clusters independently of the t-tubule-AChR trafficking pathway. Therefore we detubulated cells and looked at α dystroglycan recruitment at the cluster after agrin. In detubulated cells AChR and rapsyn were weakly clustered after 3hrs, while α dystroglycan clustering was strong and unaffected by the loss of t-tubule function (fig 6b). Therefore α dystroglycan strengthens independently of AChR and rapsyn.

Inhibition of α dystroglycan with a function-blocking antibody allowed clusters to form, but not strengthen (fig 6c), similar to previous reports (Jacobson et al 2001). Hence α dystroglycan function is required for strengthening. To discern the mechanism of α dystroglycan mediated strengthening, we looked at AChR trafficking and caveolin-3 t-tubule recruitment after α dystroglycan function blocking. We noticed that AChRs still trafficked through caveolin-3 t-tubules, however, t-tubule recruitment was blocked in these clusters. Hence α dystroglycan function is required to recruit t-tubules, the AChR trafficking and strengthening organelle, to clusters.

Figure 6.

6a

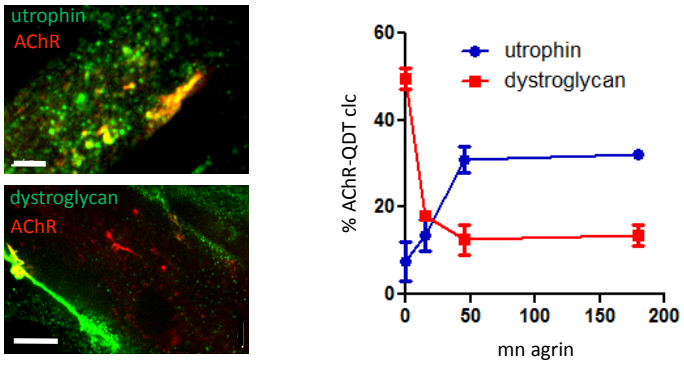

6b

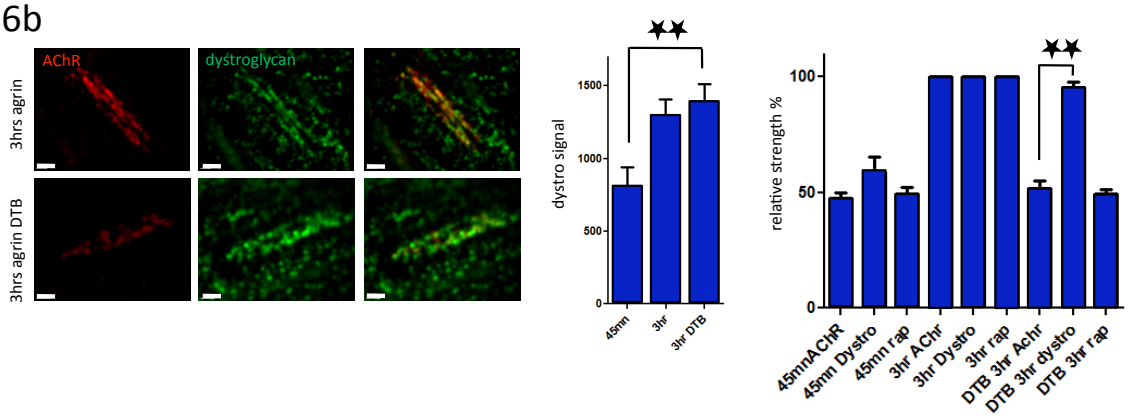

6c

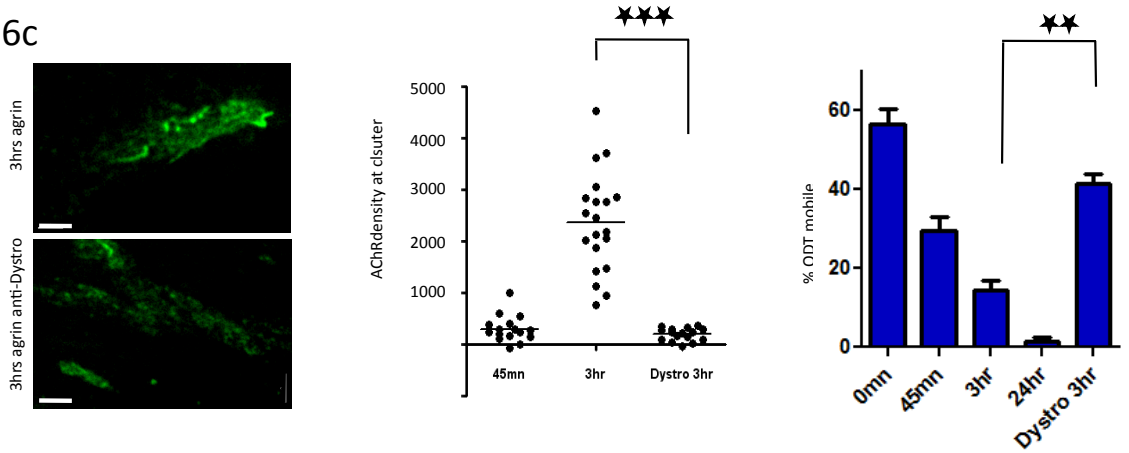

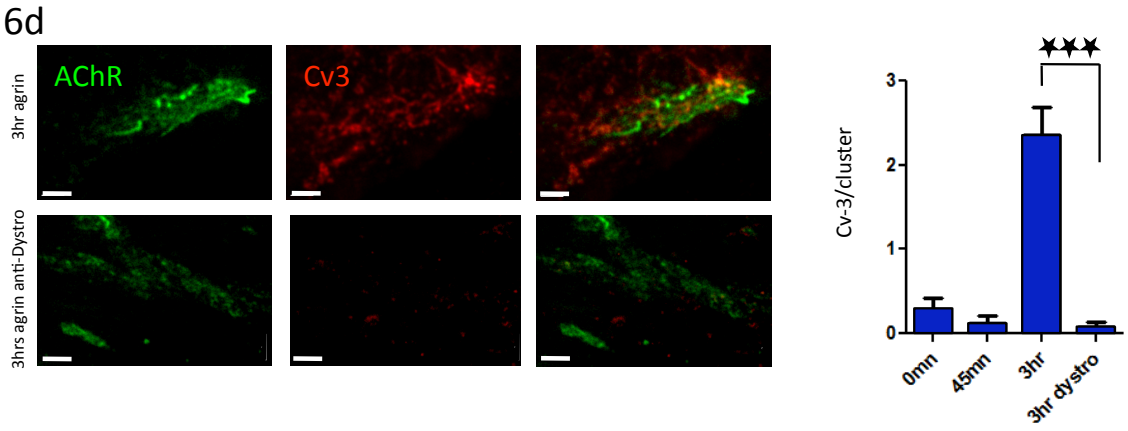

Figure 6. Dystroglycan does not package with AChR, and is required for t-tubule recruitment.
6a. Left: images of utrophin dytroglycan colocalization with non-cluster and intracellular AChR after 3hrs agrin; scale bars are 5µm. Right: quantification of pulse-chased AChR-QDTs with utrophin and dystroglycan at different times after agrin.
6b. Left: images of AChR and dystroglycan staining at clusters in control cells (top row), and detubulated cells (bottom row); scale bars are 1µm. Right: moving left to right, quantification of dystroglycan at clusters in control and detubulated cells (45mn in control versus 3hrs agrin in detubulated (DTB) cells t-test, p=0.002); quantification of relative AChR, rapsyn, and dystroglycan signal intensities, at 45mn and 3hrs agrin in control cells, and after 3hrs agrin in DTB cells (t-test,p<0.001).
6c. Left: images of AChR (green) staining in control (top) and anti-dystroglycan (bottom) treated cells; scale bars are 3µm. Right: moving left to right, quantification of AChR intensity at clusters (t-test, p=0.0006), and mobile fraction of AChR-QDTs in anti-dystroglycan treated cells versus untreated cells (3hrs agrin in control and anti-dystroglycan cells t-test, p=0.0059).
6d. Left: AChR and caveolin-3 staining in control (top) versus DTB (bottom) cells; scale bars are 3µm. Right: caveolin-3 recruitment after 3hr agrin in anti-dystroglycan cells compated to untreated cells (3hrs agrin in untreated versus anti-dystroglycan cells t-test, p=0.0005).

7. Evidence for caveolin-3 trafficking and recruitment, AChR-rapsyn packaging, Rb27b direct insertion, and AChR immobility in vivo.

Do the mechanisms we described in vitro happen in vivo? It is well documented that AChR and rapsyn densities, as well as AChR stability, increase at the NMJ over the course of a month between birth and p30 (Valenzuela et al 2011 and reviewed in Sanes and Lichtman 2001). Coincidentally, t-tubules begin formation shortly before birth, and mature over a period of weeks after birth (Al-Qusairi and Laporte 2011). Because t-tubule recruitment was correlated with and required for increased AChR density and stability in vitro, we decided to stain for t-tubules in vivo at a time when AChR density and stability increases. At p2, caveolin-3 t-tubules were not visible at AChR stained NMJS (fig 7a). At p8, caveolin-3 stain was present, but by p20 caveolin-3 was strongly intertwined with the NMJ (fig 7a). Hence NMJ caveolin-3 staining increases between p2 and p20 ($p< 0.0001$, t-test comparing p2 to p20 recruited caveolin-3), and therefore t-tubules recruitment in vivo correlates with postnatal strengthening.

We also wanted to know if AChRs traffic via caveolin-3 in vivo, as they do in vitro. Pulse-chased AChR-BTX488 in live p8 pups, increased their caveolin-3 colocalization with a peak at 45mn ($p=0.0001$, anova), which is similar to the in vitro time course (fig 7b and 3c). Furthermore, rapsyn and Rb27a colocalized with pulse-chased (60mn) AChR-BTX488 at NMJs in vivo (fig 7c), indicative of a similar packaging and exocytic mechanism found in vitro. Also, the Rb27a vesicles locate directly over the middle of NMJs (fig 7c), which suggests that the insertion is likely to be direct at the NMJ rather than periphery. Most importantly, like in vitro, surface labeled AChR traffic intracellularly to Rb27a exocytic vesicles, which are located near the NMJ.

Finally we also attempted to measure AChR-QDT mobility at NMJs in vivo to see if there is a shift towards immobility after t-tubule recruitment and trafficking, as is seen in vitro (fig 1c). Extracellular matrix was briefly shaved with collagenase to

allow QDT labeling. We only managed to get very few successful labels and traces, which were confounded by low efficiency labeling and muscle twitching, but we did see a shift towards immobility between p2 and p20 similar as that seen in vitro.

Hence caveolin-3 trafficking, t-tubule recruitment, rapsyn-AChR pre-packaging, Rb27b mediated direct insertion; and receptor mobility all follow similar trends in vivo and in vitro. The literature has well established that AChR stability increase at the NMJ at this time, and we provide some evidence that AChR-QDTs become more immobile at the NMJ at this time.

Figure 7.

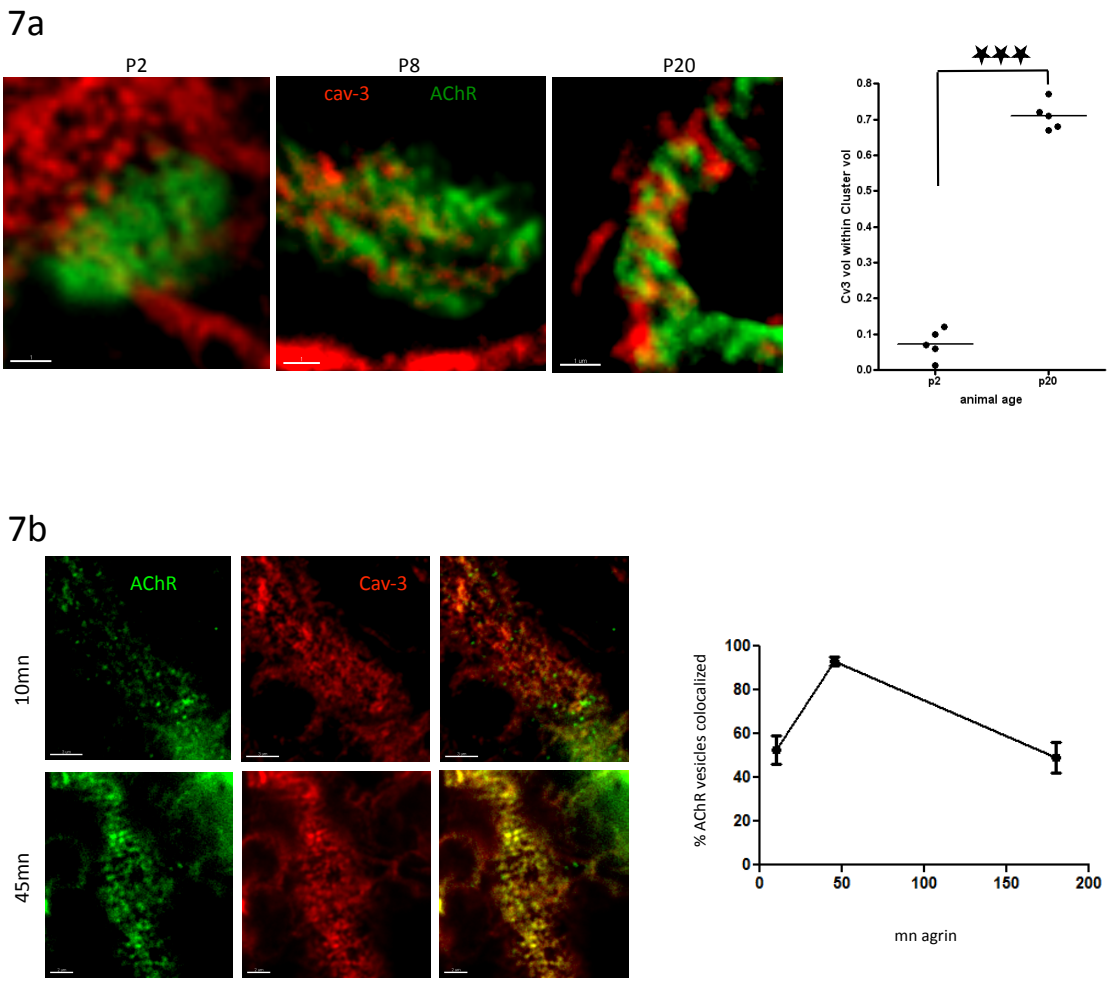

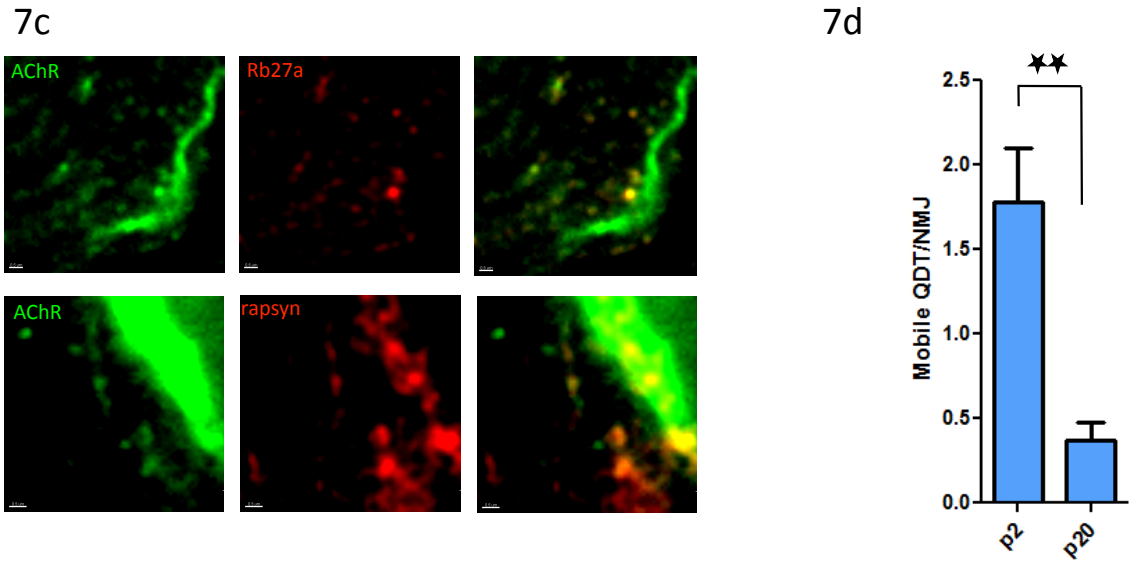

Figure 7. T-tubule recruitment, and AChR trafficking, packaging, and mobility in vivo.
7a. Left: images of AChR and caveolin-3 staining at p2,p8, and p20; scale bars are 3µm. Right: quantification of recruited caveolin-3 within the area of the cluster (t-test, $p<0.0001$).
7b. Left: images of pulse-chased AChR-BTX488 after 10mn and 45mn chase, and then stain for caveolin-3, in p8 pups; scale bars are 3µm. Right: quantification of pulse-chased AChR-BTX488 vesicles that colocalize with caveolin-3.
7c. Images of pulse-chased AChR-BTX488 colocalizing with rapsyn and Rb27b after 60mn chase in live p8 pups; scale bars are 0.5µm.
7d.Quantification of mobile AChR-QDTs at p2 and p20 NMJs (t-test, $p=0.0017$).

8. Evidence of transport packages at strengthening synapses in the CNS.

Does prepackaging happen at other synapses, for example at the CNS? Above we demonstrated AChR-rapsyn packaging by pulse-chasing surface labeled AChRs, and then fixing and staining for rapsyn. We found that as receptors trafficked through the cell, they increased their colocalization with rapsyn. Therefore we wanted to perform an analogous pulse-chase of receptor and scaffold stain in the CNS.

In the CNS, Glur1 interacts with between 1 and 4 stargazin molecules (Kim et al 2010), analogous to how AChRs interact with either 1 or 2 rapsyns. After LTP induction, Glur1 becomes trapped and immobilized in the postsynapse via stargazin (Opazo et al 2010), similar to how AChRs are anchored to the postsynaptic cytoskeleton via rapsyn after agrin. Therefore we wanted to test if glycine induced LTP would increase the amount of stargazin per Glur1, similar to how agrin increases the amount of rapsyn per AChR (fig 5c and Moransard et al 2003).

Before we pulsed-chased surface labeled AChR-BTX and found that as AChRs trafficked, they increased their colocalization with rapsyn inside the cell. Therefore we pulse-chased surface Glur1 labeled with anti-Glur1 (n-terminal antibody) and rhodamine dextran (RD), fixed and stained to see if Glur1-stargazin colocalization increased. We found that after 5mn LTP there was little colocalization of Glur1-stargazin inside endocytosed RD, whereas after 20mn there was a dramatic increase in colocalization (fig 8a). We confirmed this result by surface labeling GluR1 in live cells after 0 or 20mn LTP, then fixing and staining for intracellular Glur1 and stargazin. Using QDTs as the intracellular secondary probe, we found that percent of QDT-stargazin colocalizations increased from about 60 to 90% ($p < 0.001$, t-test) (fig 8b). Hence after LTP intracellular Glur1-stargazin increases its colocalization inside the cell, which could reflect an increase interaction of stargazin and Glur1 induced by LTP

Figure 8.

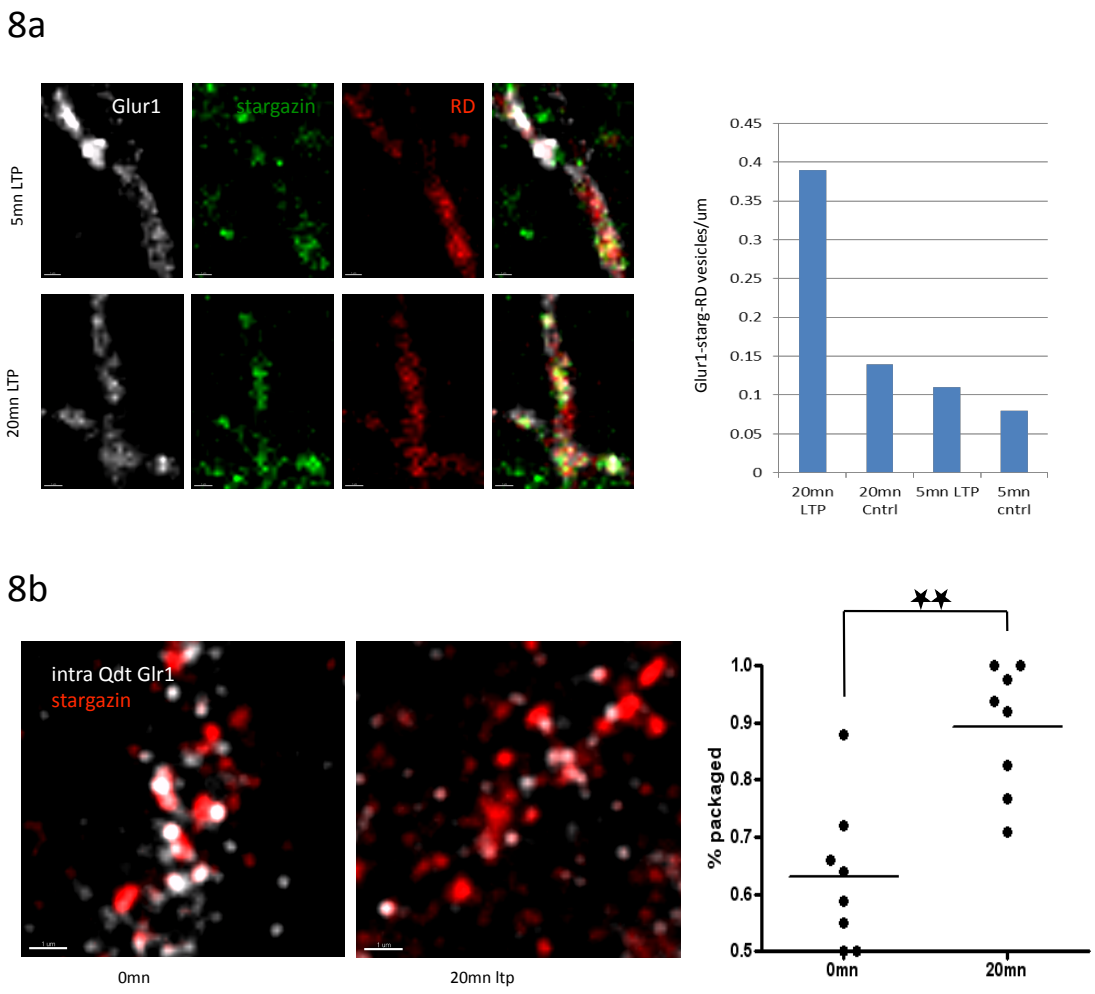

Figure 8. Induced Glur1-stargazin packaging.
8a. Left: images of Glur1, stargazin, and rhodamone dextran (RD) staining after labeling surface Glur1 with anti-Glur1, washing and then stimulating wth glycine 5mn and 20mn in the presence of 5mn RD; scale bars are 1µm. Right: quantification of the number of Glur1-stargazin colocalizations within RD vesicles, per µm. The 20mn LTP significantly differs from the other conditions, but this preliminary result has not yet been repeated.
8b. Right: staining for stargazin and intracellular staining for glur1-QDT after surface labeling with anti-Glur1 prior to fixation 0 and 20mn after LTP; scale bars are 1µm. Right: quantification of intacellular Glur1-QDT colocalizing with stargazin before and after 20mn glycine stimulation (t-test, $p < 0.001$).

Supplemental Figures.

Supplemental figure 1.

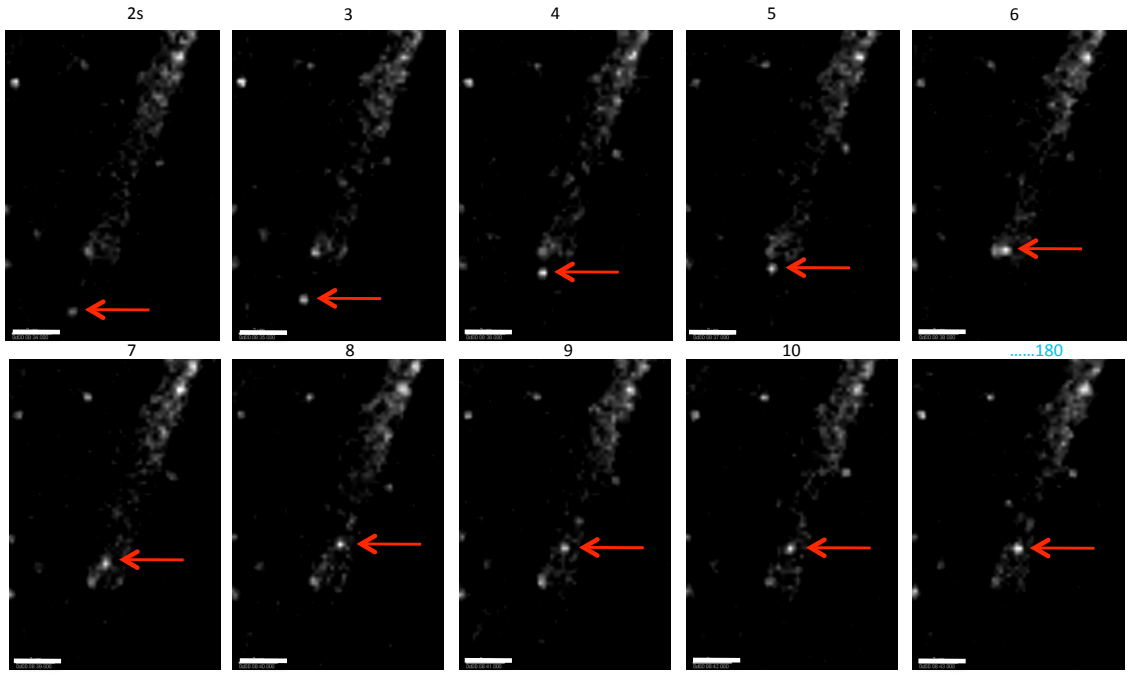

AChR-QDTs (white) imaged every second, near a cluster (white) on the side of the cell. Red arrows indicate the trajectory of the QDT, which is a straight line to the cluster and then immobility. Error bars are 2um.

Supplemental figure 2.

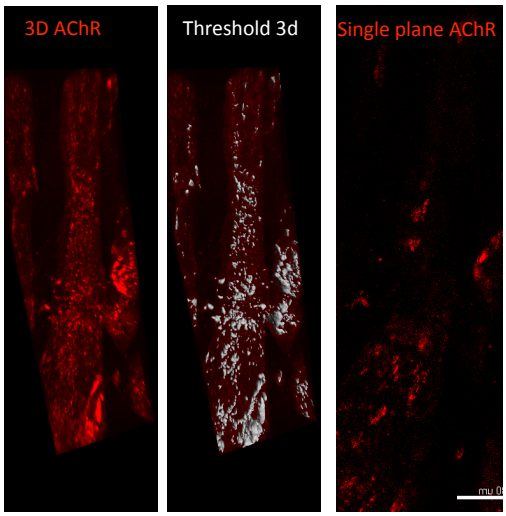

Left, AChR signal was reconstructed in 3D, and then thresholded (white middle) to reveal where intracellular AChR was located in the cell. The single plane image (right) is from the same cell, and shows where the clusters are relative to the intracellular accumulations. In this example there is a large accumulation at the bottom of the cell, and much less at the top. In the same cell, clusters are more AChR dense at the bottom of the cell than the top. Hence the density of AChR, or cluster strength varies with the presence of the intracellular accumulation (scale bar is 10um).

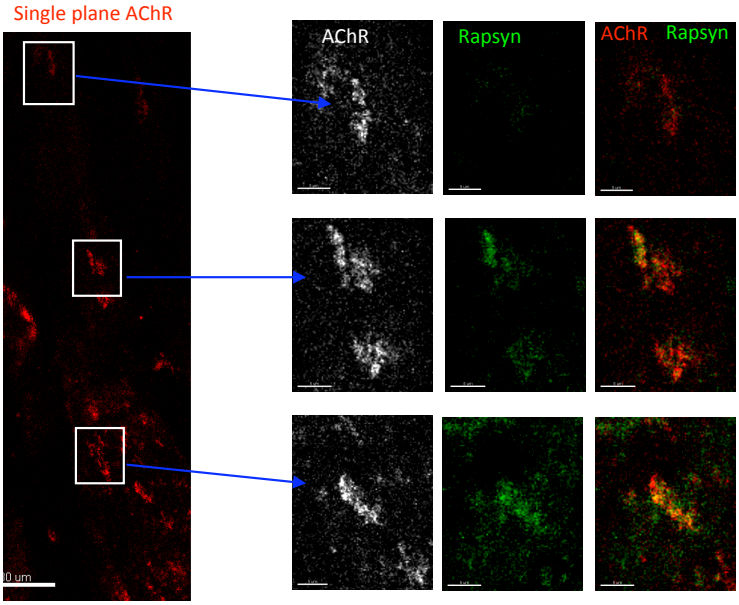

Above left, the same single plane image as above. Right, the same cell fixed and stained for rapsyn. Again revealing a correlation between the proximity of the intracellular accumulation and the strength of the cluster, because there was more accumulation at the bottom of the cell where clusters have more rapsyn (scale bar is 1um).

Supplemental figure 3.

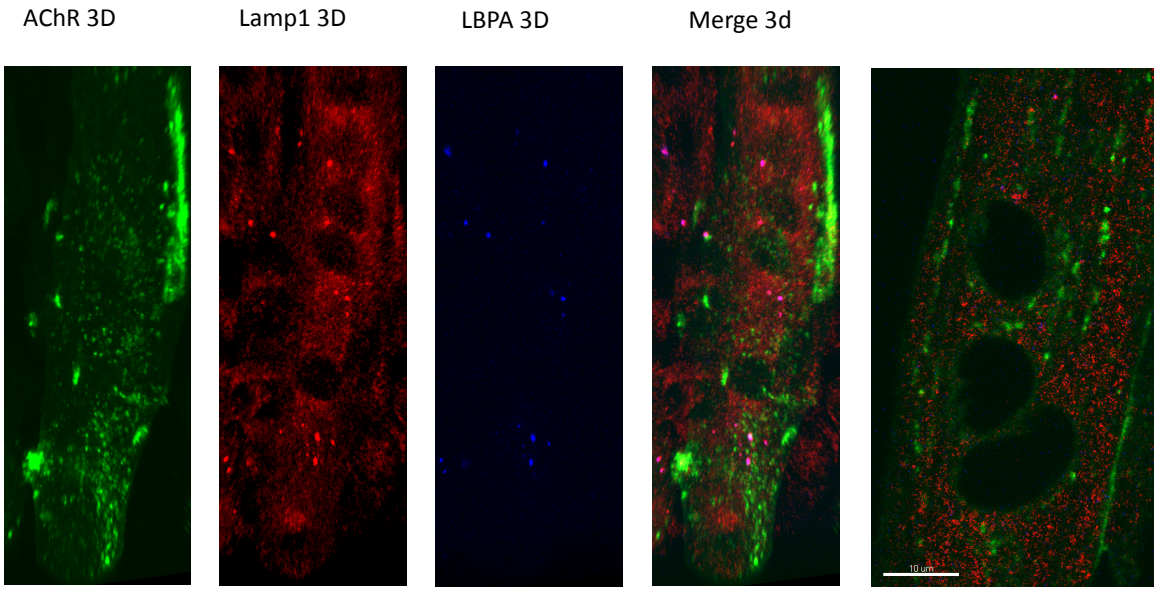

Intracellular AChR accumlations after 3hrs agrin do not colocalize with Lamp1 or LBPA, markers of late endosome and degradation. Left are 3D reconstructions, and furthest right is a single plane image (scale bar is 10um).

Supplemental figure 4.

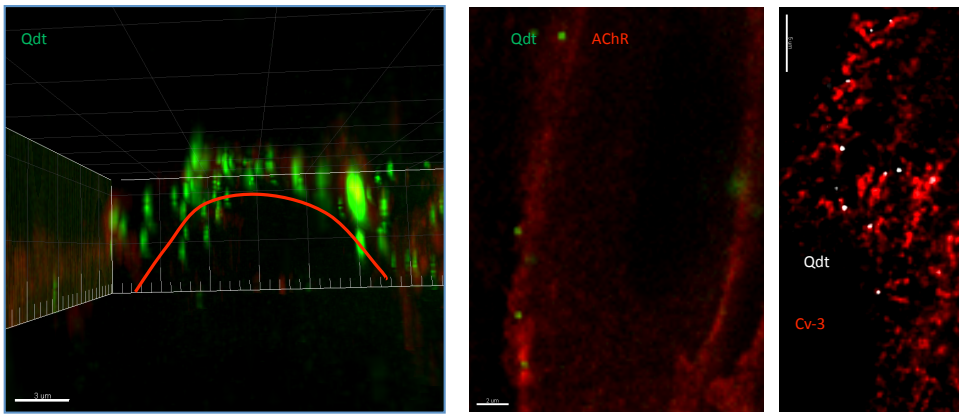

QDTs only label surface, but can traffic into intracellular compartment. Above left, 3D reconstruction of QDT labeling; view is looking through the myotube, whose peripheral border is marked with the red line; error bar is 2um. Middle, single plane view of QDT labeling showing that QDTs only label the surface periphery; error bar is 2um. Right, single plane image of pulse-chased QDTS colocalizing with caveolin-3 in the middle of the cell, not the periphery; error bar is 1um.

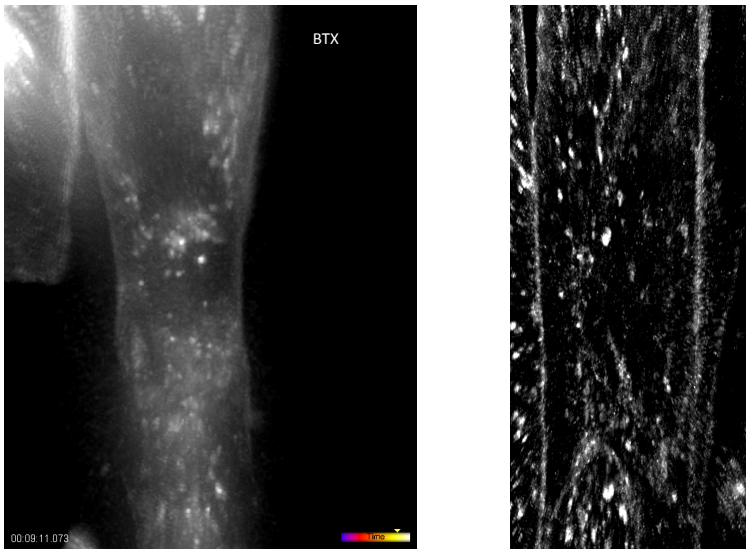

BTX surface label also labels surface accessible, intracellular compartment. Unlike the QDT label, BTX labels AChRs within the periperhy of the cell. Left is a 3d reconstruction and right is a single plane; both images reveal labeling well within the periphery of the cell, which is in contrast to the QDT label above.

Supplemental figure 5.

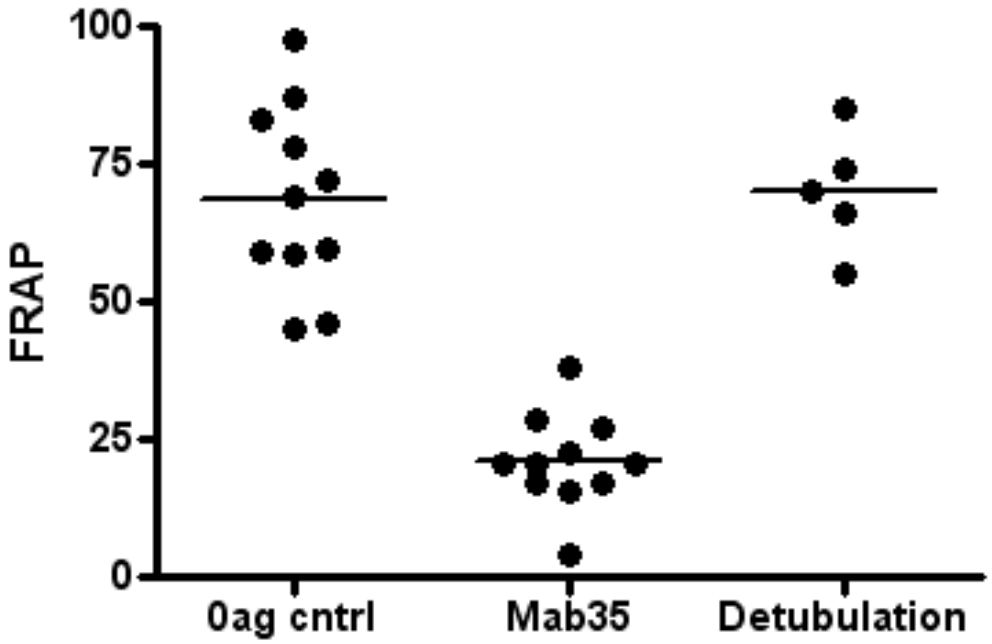

Detubulation does not affect the fast FRAP at weak clusters. 7mn FRAP was performed on weak clusters without agrin (left). Treatment with detubulation had no affect on the FRAP, whereas crosslinking with the AChR antibody Mab35, reduced FRAP ($p<0.0001$).

Supplemental figure 6.

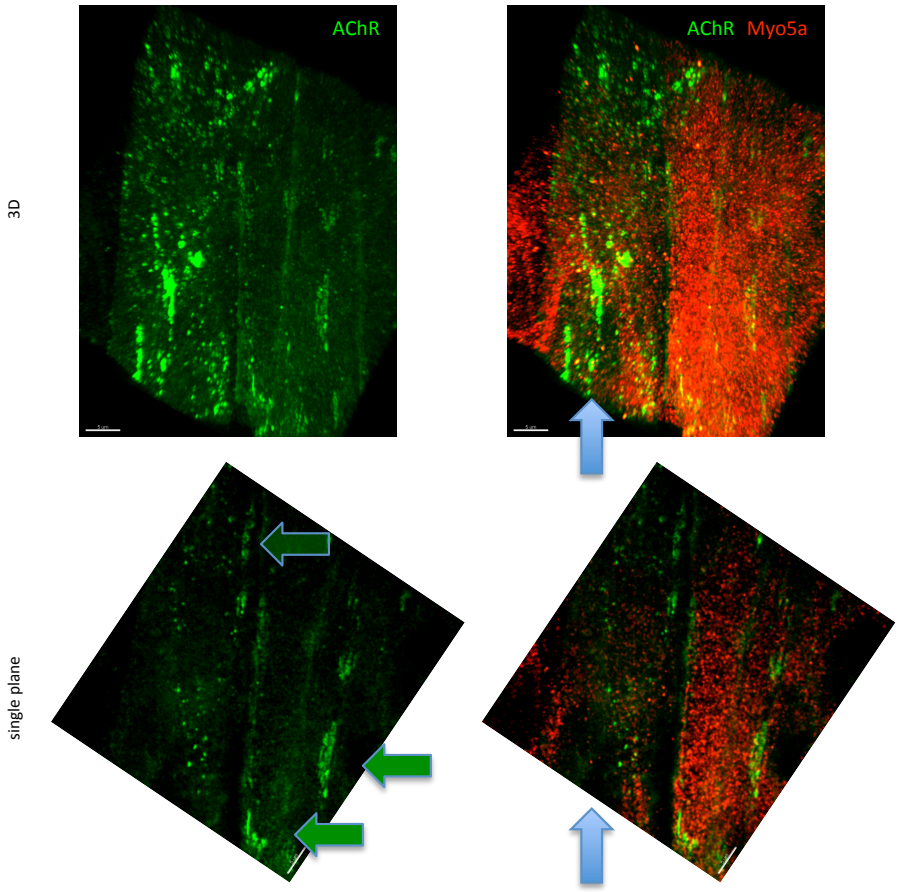

Evaluation of MyosinVa knockdown with posthoc staining. Cells were treated with lentiviral transduction particles to knockdown myosinVA, and staining was evaluated by posthoc staining for myosinVa. In the example above, the left most cell (blue arrow) has much less myosinVA staining than cells on the right (top 3D images)(scale bar = 5um). In the single plane images it is also clear that clusters formed (green arrows) in all cells but only strengthened in cell with high levels of myosinVA (scale bar = 5um). Knockdown cells were identified by having myosinVA staining near background levels.

Supplemental figure 7.

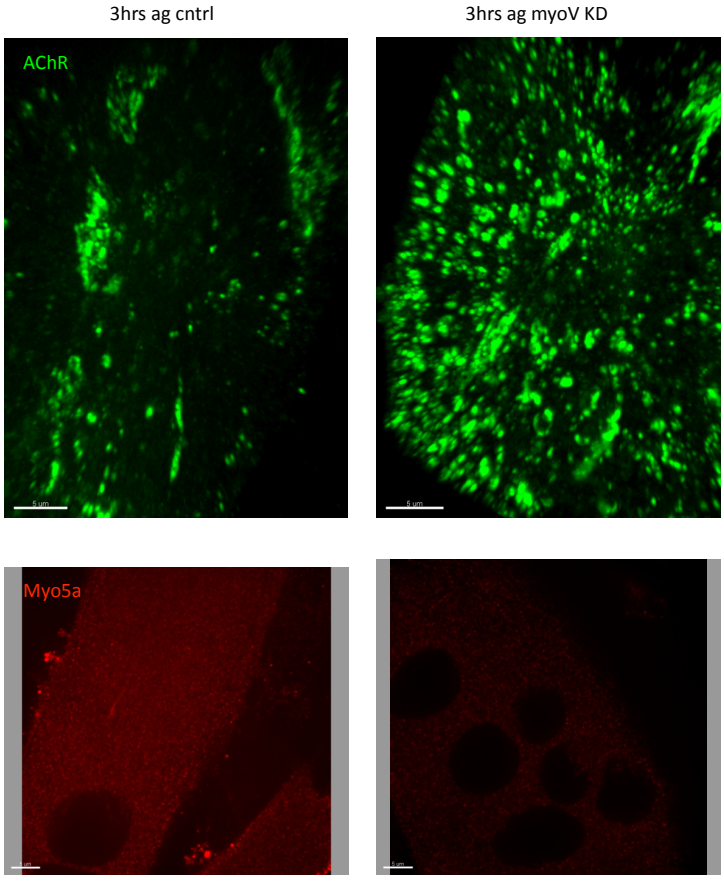

Above, cells in the same dish treated with lentiviral transduction particles against myosonVA. Left, control cells had little knockdown (bottom left panel, staining myosinVA), and formed clusters; some intracellular accumulation is apparent (scale bar = 5um). In knockdown cells (right), dramatic intracellular accumulations were seen throughout the cell. These intracellular accumulations in knockdown cells were often bigger and brighter than clusters, as seen below (scale bar = 3um). The images below are blow ups from the cells above. They were imaged on the same day, and in the same dish, so their signal is comparable.

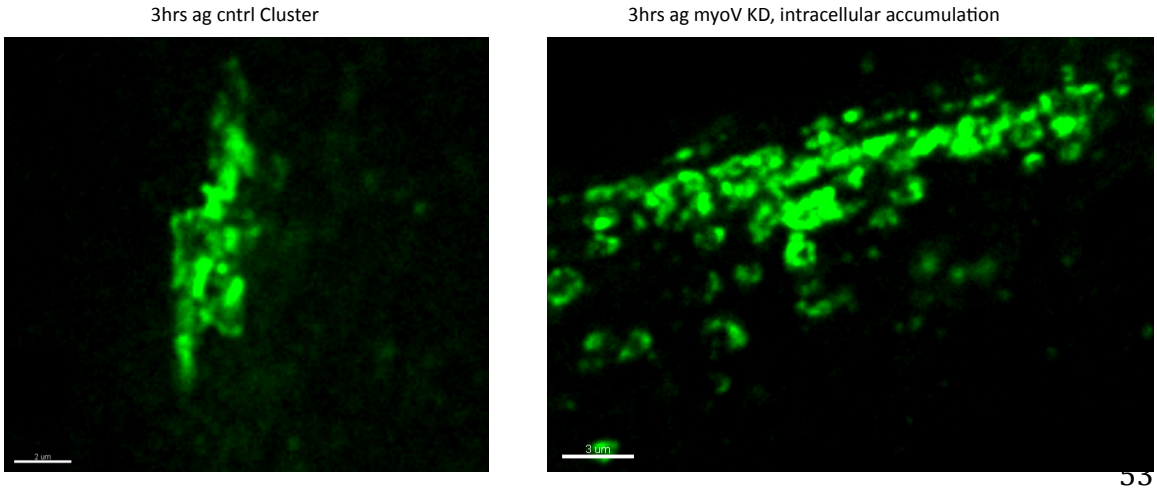

Supplemental figure 8.

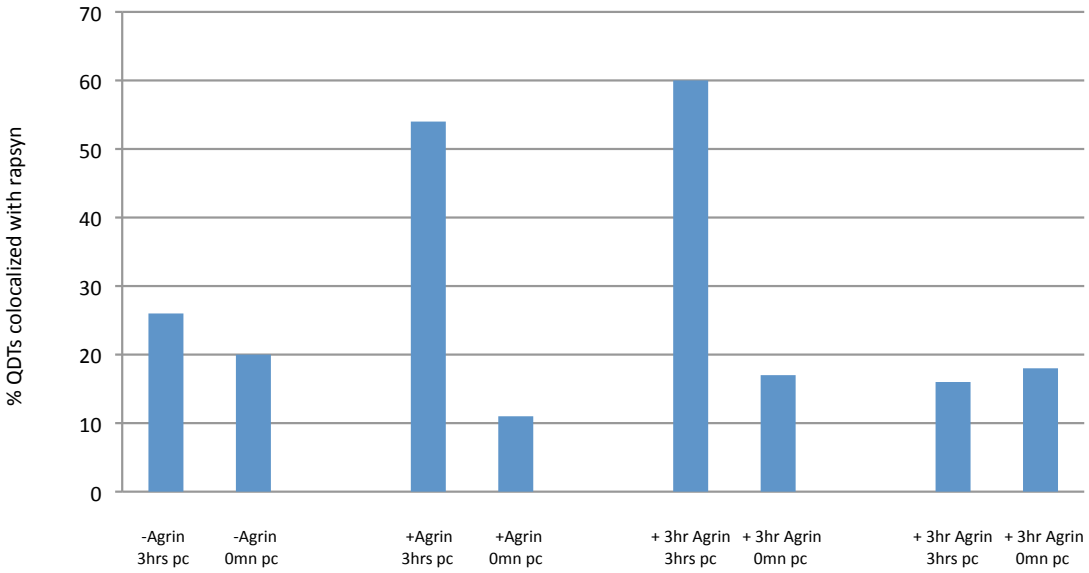

Surface labeled AChR-QDTs were pulse-chased for 3hrs or 0 hours in the absence of agrin (left most bars), just after agrin (middle left bars), after 3hrs agrin (middle right bars), or after 24 hrs agrin. After chase, the cells were fixed and stained for rapsyn. The y-axis represent the percentage of pulse chased QDTs that colocalized with rapsyn after fixation.

Supplemental figure 9.

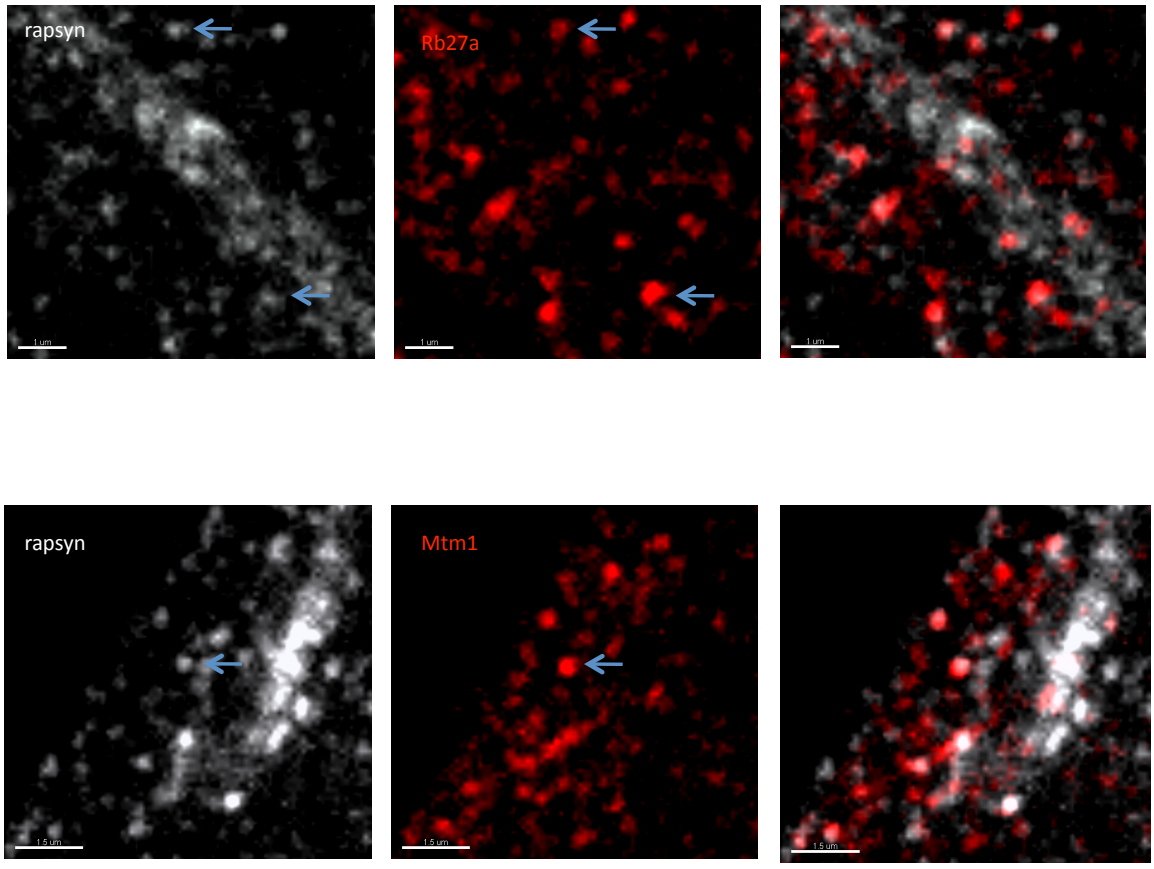

Rapsyn colocalizes with Rb27a and MTM1 vesicels near clusters. Above, cells were treated with 3hrs agrin, fixed and stained for rapsyn and Rb27a. The cluster is visible in the rapsyn channel running diagonally across the field of view. Colocalizations are exemplified with small blue arrows. Scale bar is 1um. Below, is the same as above except staining for MTM1 staining and scale bars are 1.5um.

Discussion.

In this thesis we showed diffusion-trapping at weak clusters but insertion of immobile AChR at strong clusters, using FRAP and single particle tracking. Surface AChRs endocytose, traffic via caveolin-3 t-tubules, package with rapsyn, and then insert immobile at clusters in a myosinVa dependent manner. This intracellular trafficking and packaging is required for the strong state of assembly at the cluster, consisting of high density AChR and rapsyn, as well as AChR immobility. We also find that α dystroglycan function is required for the postsynaptic recruitment of t-tubules, which traffic, package and insert AChRs. These findings provide a new model of postsynaptic receptor addition in which receptors endocytose, package with scaffold, and insert immobile at the postsynapse.

The diffusion-trap model of postsynaptic receptor addition has predominated since its inception, over 35 years ago (Axel et al 1976, and Opazo and Choquet 2011). Here I provide evidence for a new model of postsynaptic receptor addition: the 'preassemble-insert model', involving 1) receptor endocytosis, 2) intracellular receptor-scaffold preassembly, and then 3) targeted insertion of immobile receptors into the postsynapse (fig 3.1).

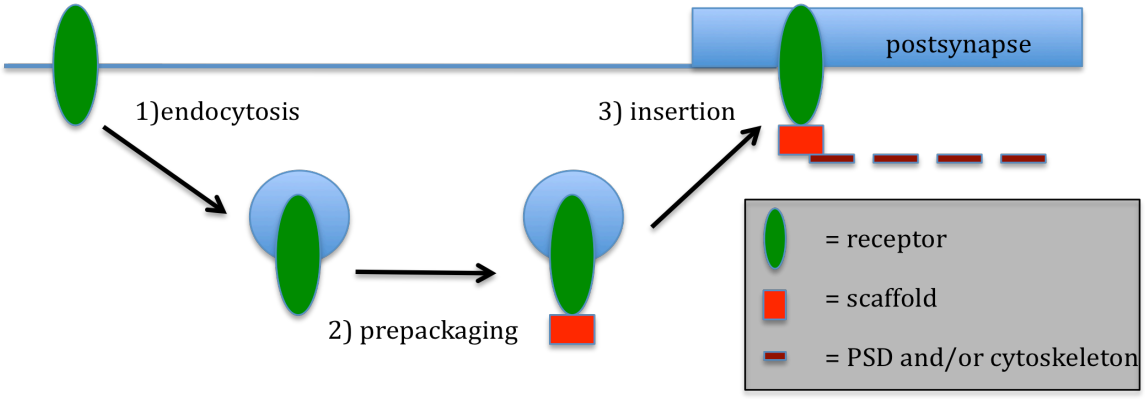

Figure 3.1 The preassemble-insert model.
In the three-step model, intracellular receptors (green oblongs inside blue circles) are 1) endocytosed, 2) packaged with scaffold, and 3) inserted directly into the postsynapse as an immobile receptor-scaffold package.

Below I will discuss how diffusion-trapping compares to preassembly-inserting, the significance of t-tubule recruitment and function in postsynaptic strengthening, how these data might generalize to the CNS and other cell-cell junctions, and propose α dystroglycan as a slot molecule.

Brownian Diffusion and trapping versus targeted insertion of immobile receptor.

The most commonly reported mode of receptor trafficking into a postsynapse is diffusion followed by trapping (Renner et al 2008). Using single particle tracking and FRAP we showed AChR diffusion into weak clusters but little or no diffusion into strong (fig 1a and 1c). If there is no diffusion into strong clusters, but strong clusters are full of immobile receptors, then insertion of immobile receptors is a possible mechanism of receptor addition that satisfies the limiting conditions of no diffusion and high immobility. We used single molecule tracking to demonstrate the insertion of immobile receptors, without a detectable diffusion step (fig 2b). Surface versus inserted labeling showed that insertion dominates the addition of AChR to strong clusters, whereas diffusion contributes relatively little (fig 2c). Finally, the FRAP and QDT tracking data (fig 1a and 1c) suggested that strong clusters act as diffusion barriers, because there was little or no diffusion into or within strong clusters.

This is the first direct evidence of immobile insertion at any cell-cell junction. Direct insertion of immobile receptor is intuitively appealing because it is specific and targeted, whereas Brownian diffusion is random and not targeted. However, there are different advantages and disadvantages to both Brownian diffusion and targeted insertion of immobile receptors.

Diffusion has the advantage of being fast. Receptors can diffuse into postsynapses within seconds to a few minutes (fig 1a and Opazo et al 2010), whereas endocytosis, intracellular transport, packaging, and then insertion might take tens of minutes (fig 2a). Hence diffusion might act fast and local, whereas targeted insertion might act slow and far. While it is clear that there are many examples of synapses and cell-cell contacts that rely on diffusion based transport (Renner et al 2008), we propose that there might also be cell-cell junctions and scenarios unsuitable for diffusion-based transport.

Many synapses and cell junctions might not be permeable to diffusion-based transport.Therefore targeted insertion may be favorable over diffusion at such synapses or junctions. The NMJ is a very densely packed synapse, estimated to have 20,000 AChRs per square um, plus many other transmembrane molecules at similar densities (Kummer et al 2006). High density of protein alone can act as a diffusion barrier, in a biophysical process called 'molecular crowding' (Ryan et al 1988), but also consider that many of junctional proteins are in large complexes and immobile. Therefore diffusion into a densely packed synapse with a high immobile fraction of interconnected proteins is very unlikely, purely because there is no space to diffuse. A high density of immobile proteins could well act as a diffusion barrier at the NMJ or other synapses. Furthermore there is the possibility that actin driven membrane deformation, such as that seen at NMJ folds (Kummer et al 2006), as well as specific barrier proteins (Hu et al 2010), can also act as diffusion barriers.

The high protein density and immobility at the NMJ might be considered unique to this specific synapse, however this is not the case. There are estimates of over 1000 AMPARs per micrometer in CNS synapses, and there are very recent reports of high percentage receptor immobility in the synapse. Most notably, bleaching subdomains within the PSD reveals that there is no diffusion of AMPARs within the PSD, but there is a high immobile fraction (Kerr and Blanpied 2012). This scenario of 1) a high AMPAR immobile fraction and 2) no AMPAR diffusion, is the exact scenario that is not amenable for diffusion. This is also exactly the scenario we propose for direct

insertion of immobile receptor. However, the authors propose that receptors still laterally diffuse into the periphery, become immobile, and then 'treadmill' (driven by actin) into the center as a presumable Glur1-stargazin-PSD-95 complex. This model seems paradoxical because treadmilling is still a form of lateral mobility, and the data in the paper shows immobility within the PSD.

Our FRAP and single molecule data show that receptors are initially mobile in weak clusters, and that strong clusters act as diffusion barriers: receptors rarely diffuse into and within strong clusters (fig 1a and 1c). Whether this diffusion barrier is due to synaptic protein density alone, a high immobile fraction, crosslinking with the cytoskeleton, membrane deformation, or a specific protein barrier is unknown. Many other cell-cell junctions have high protein densities, high immobile fractions, deformed membranes, and other diffusion barriers (Simek et al 2009 (connexins, gap junction), Adams et al 1998 (E-cadherin), Causeret et al 2005 (N-cadherin) Nachury et al 2010 (ciliary membrane) (Rasband 2010 axon initial segment)). It is therefore possible that direct insertion of immobile protein occurs at these junctions. Furthermore the trend of starting as a diffusion-trap with mobile protein, and then switching to an immobile state, is common at many of these junctions and in our data. Hence a shift from protein mobility to immobility and from diffusion-trap to preassemble-insert or immobile insertion might be generalized at cell-cell junctions.

Targeted insertion might also be favorable in regard to the slot hypothesis (Xu 2011), which assumes a limited number of physical spaces, or 'slots', available for receptors; analogous to car parking spots in a parking lot. By this metaphor, imagine if a car park is very full, there is a traffic jam within the car park, and moving forward is as rare and difficult as finding a parking spot. In this scenario, it would be ideal if a crane lifted cars and inserted them into available spots, and also if the crane would remove cars to create empty spots. However if there are many free spaces, and there is no traffic within the car park, then it is surely faster if cars drive into free spots; and it is surely a waste of time and energy to be moved into a free

spot by a crane. Hence the efficiency of receptor slotting is limited by the traffic around the slot. Insertion is optimal at a high immobility junction, whereas diffusion is better when there is high mobility.

This car park metaphor is also interesting because it raises the question of the geometry of the car park, or slots. If all the parking spots, or postsynaptic slots, are side by side and all the receptors are immobile, then insertion might be favorable (fig 3.2 left), because diffusion is blocked by molecular crowding. However, if the parking spots, or slots, are spaced out with plenty of room for driving or diffusion, then diffusion might be favorable (fig 3.2 right). The spacing of the slots might determine local mobility or immobility. Hence, targeted insertion might be a more efficient way to add receptor to synapses that have densely packed slots, large surface areas, and a high immobile fraction. Diffusion would be better if there is space to diffuse, and if there are many slots accessible to diffusion (fig 3.2).

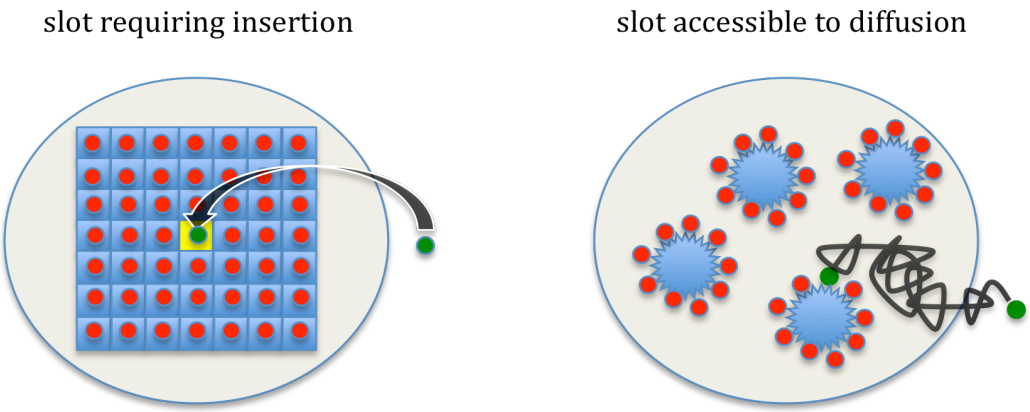

Figure 3.2 Slot geometries favoring insertion or diffusion
If slots are filled with immobile protein, then the geometry of slots might vary according to the mechanism of trafficking. On the left, all the slots (blue squares) are occupied by immobile receptors (red dots). Therefore the addition of extrasynaptic receptor (green dot) to a vacant slot in the middle of a grid of slots might require insertion. However if diffusion is the mode of trafficking, then slots might have different geometries amenable to diffusion. On the right, slots islands (blue) are organized in a circular arrangement, and there is much space in between slot islands for an extrasynaptic receptor (green dot) to diffuse into and occupy.

Strengthened synapses in the CNS and PNS persistently contain receptors immobilized via a scaffold or PSD connection (Renner et al 2008). It is tempting to

speculate that immobility and insertion might serve two functions. Firstly, immobile receptors might better bind neurotransmitter receptor, either because they are not moving, or because they undergo a conformational change. Secondly, immobility and immobile insertion might allow for a higher density or packing order than diffusion trapping (Gervasio et al 2007). In the experiments where strengthening was blocked, diffusion-trapping still occurred but clusters did not become as densely packed as strengthened clusters despite having the same amount of time to do so. Hence immobility might be a better way to make the synapse stronger because it can create a higher density of receptor than a diffusion-trap. In the CNS diffusing receptors become immobile after trapping. It would be interesting if diffusing AChRs could also be immobilized by ACh or electrical stimulation, while insertion is blocked, to see if high density packing is achieved.

Diffusion is unlikely to act over long distance. Using Einstein's equation for diffusion in one dimension ($x=2Dt$, where x is the distance, D is the diffusion coefficient, and t is time) and the diffusion coeffcients from the QDT data ($D=.1\mu m^2/s$), it is possible to calculate how long it would take a receptor to diffuse the length of a myotube (100um) into a cluster. Interestingly it would take about 8hours to diffuse 100um in a straight line, the same time it takes for clusters to fully form. Diffusion in a straight line might sound unrealistic but so called 'diffusion tracks' could allow for such directed and linear diffusion (Shafrir et al 2000). However, we never saw diffusion track movement outside of clusters before or after agrin, only Brownian motion. Extrapolating the same Einstein equation to the surface area of a myotube (about $4700um^2$) it would take over 2 weeks for distant AChRs to diffuse into the cluster relying on Brownian motion, and statistically it could take much longer. Brownian motion is random and the membrane is approximately evenly distributed with AChR, outside of clusters. Hence only receptors nearby the postsynapse are likely to diffuse in.

Trafficking through the t-tubules, and t-tubule polarization towards the cluster does create spatial and temporal specificity for insertion. Interestingly it also allows for a

factory mill style processing of AChRs before insertion. Caveolin-3 is enriched in src kinases, which phosphorylate AChR and allow for the addition of rapsyn (Mittaud et al 2001). One can imagine that as AChRs traffic through specific compartments en route to the cluster, they receive specifc modications, which ultimately determine the stability of the receptor and state of assembly at the cluster.

The caveolar trafficking route to the synapse that we have described is complex, involving transcytosis. Receptors are initially inserted to the surface membrane, endocytosed to the t-tubule/caveolar system, and then finally inserted at the cluster. One interesting question about transcytosis is: what is the functional reason for indirect trafficking, and why pay the high-energy cost of additional trafficking? Here we show that this indirect intracellular trafficking is required for receptor immobility and synaptic strengthening. Hence the function of this indirect trafficking is the assembly of a receptor complex that has a state specific to immobility.

This is the first report of immobile receptor insertion at a synapse, or any cell-cell junction. We propose that this mechanism would be energetically and temporally favorable at cell-cell contacts with unfavorable conditions for diffusion, such as diffusion barriers or high concentrations of immobile protein.

Agrin induced AChR trafficking via t-tubules.

Perhaps the most striking result in this thesis was the massive intracellular accumulation of surface AChRs after agrin (fig 3a). These intracellular accumulations were often larger and more densely packed with AChR than clusters. Furthermore, it was surprising that AChR trafficking via t-tubules was required for cluster strengthening but not formation (fig 4a). Therefore it was important to characterize this novel trafficking pathway.

We found that AChRs traffic from the surface, via an intracellular compartment, before inserting at the cluster. Using an immunostaining screen and AChR-QDT pulse-chasing (fig 3b), we found that AChRs traffic through specific t-tubule compartments with specific kinetics: early and fast through dysferlin, early and slow through cavoelin-3, and late and long in MTM1 (fig 3c). AChR-QDTs also colocalized with rhodamine dextran after agrin (fig 3c), implying endocytosis. T-tubule incapacitation and diversion of caveolin-3 trafficking (by detubulation and APOE4 treatment) prevented cluster strengthening and AChR insertion (fig 4a and 4d). Hence t-tubule trafficking is required for cluster strengthening.

This is a novel report for t-tubules as a trafficking organelle involved in AChR clustering. T-tubules are most commonly known for their role in calcium signal propagation throughout the muscle after depolarization at the NMJ, and less is known about their roles in trafficking (Al-Qusairi and Laporte 2011). This study proposes that dysferlin, caveolin-3, and MTM1 might mark early, middle, and late t-tubule trafficking compartments. However we cannot exclude the possibility of recycling or other intermediate trafficking steps. AChRs might not traffic directly between these compartments (fig 3c). We can conclude that a large percentage of surface AChR was trafficked to specific t-tubule compartments at specific times (fig 3c schematic), and we later show that this trafficking is required for cluster strengthening (fig 4a and 4d).

The focus of this part of the study was to make the initial characterization of an unknown trafficking system. The finer details of intra t-tubule transport will take time to elucidate. It is important to note that we define a trafficking axis of dysferlin-caveolin-3-MTM1, because human mutations to these genes all cause the same type of disease: limb girdle muscular dystrophy (LGMD) (Al-Qusairi and Laporte 2011). It is not known if AChR trafficking or cluster strengthening plays a role in LGMD pathology, but this study suggests that possibility. If there was a role for synapse strengthening or AChR trafficking in LGMD it would be difficult to untangle from other LGMD phenotypes such as defects in excitation-contraction coupling, t-tubule

formation, and membrane repair. Even if AChR-t-tubule trafficking is not involved in LGMD, it may be useful to have identified a potential early, intermediate, and late trafficking compartment in t-tubules.

APOE4 pretreatment misdirects AChR trafficking from caveolin-3 to MTM1 after agrin (fig 4c), and is therefore a valuable tool to study the role of AChR-caveolin-3 trafficking. We found that cells pretreated with APOE4 still formed clusters, but did not strengthen (fig 4d). It is tempting to speculate that, as a LRP4 ligand, APOE4 might attenuate LRP4 signaling similarly to LRP4 knockdown. However, it is unknown how APOE4 is affecting the LRP4 signal in this context, and it is not clear if these results are comparable to LRP4 knockout studies, which found reduced clustering (Zhang et al 2008). APOE4 treatment may well be different than knocking down LRP4. We were able to specifically detect a strong inhibition of caveolin-3 trafficking after APOE4 treatment. We suggest that the results of APOE4 treatment on clustering are indicative of this caveolin-3/t-tubule inhibition, because they are very similar to the detubulation results. It would be interesting to see how the other APOE splice variants affect AChR trafficking and clustering. Finally, APOE4 is better known for its deleterious role in Alzheimer's disease (Bu 2009). However, it was also recently shown to inhibit motor neuron regeneration (Comley et al 2011), and it is tempting to speculate a postsynaptic role. While these results do not directly address Alzheimers or regeneration, it may be of interest that APOE4 misdirects a neurotransmitter receptor trafficking pathway that is involved in synaptic strengthening.

Postsynaptic recruitment of t-tubules and ER based calcium stores.

We found that strong clusters recruit t-tubules after agrin (fig 3d), and that recruitment depended on α dystroglycan function (fig 6d). This is an important result because it shows that t-tubules (calcium handling and ER related machinery) are recruited to the postsynapse via an adhesion molecule, α dystroglycan. The t-

tubules, together with muscle ER, are known to propagate calcium signals throughout the muscle after depolatization at the NMJ. We demonstrated a novel role for t-tubule function in trafficking AChRs to strengthening synapses, beyond their classical calcium role. Furthermore we provide a novel function for α dystroglycan in t-tubule recruitment to the cluster, to strengthen the cluster.

Many strong and high fidelity synapses recruit ER, or organelles like it that propagate calcium signals, such as hippocampal mossy fibers, cerebellar purkinje cells, and the NMJ (Harris and Weinberg 2012 and Hezel et al 2010), but very little is known about how these postsynapses recruit such organelles. α Dystroglycan might also recruit ER at these CNS synapses because it is expressed there (Satz et al 2010 (mossy finers) and Tian et al 1996 (purkinje)), and because it is known to interact with synaptopodin, an actin bundling protein that recruits spine apparatus (SA) (Patrie et al 2002). It would also be interesting to look at dendrites that have variable ER recruitment (e.g. in CA1)(Holbro et al 2009) to check if presence of ER correlates with dystroglycan staining.

It is novel that recruited t-tubules function in trafficking and packaging of surface AChRs on their way to the cluster. NMDAR and AMPARs have been observed in SA (Racca et al 2000), but the regulation of receptor trafficking in the SA is unknown. NMDAR-scaffold packages have also been found in dendritic ER (Jeyifous et al 2007), but whether surface NMDARs can be cycled through this pathway is unknown.

Organelles and cell adhesion molecules are also postsynaptically recruited (McAllister 2007), and the interplay, order, and interdependence of recruitment are interesting and complicated to unravel. Here we show that α dystroglycan can cluster independently of the t-tubule pathway (fig 6b). Furthermore, α dystroglycan recruits t-tubules, which are in turn responsible for the addition of receptors to the strengthening synapse. Therefore we propose the model that cell adhesion

molecules, like α dystroglycan, recruit calcium handling organelles, like t-tubules, to strengthen postsynapses. This is a similar model to Sytnyk et al who showed that NCAM recruits TGN to developing synapses.

In summary, we show adhesion dependent recruitment of calcium handling machinery, the t-tubules. Recruited t-tubules strengthen the synapse by increasing the number and density of AChR in the postsynapse, and by propagating calcium signals after depolarization.

Preassembly of receptor-scaffold complexes at intracellular vesicles.

We found that pulse-chased AChR-QDTs increased their colocalization with the scaffold molecule rapsyn (fig 5c). When exocytosis was blocked by myosinVa knockdown, we found that rapsyn increased its colocalization with AChR inside the cell, but not at the cluster (fig 5b). When caveolin-3 trafficking was blocked, the AChR-QDT colocalization with rapsyn did not increase (fig 4a and 4d). Therefore AChR-rapsyn assembly occurs inside the cell, before insertion at the cluster (fig 3.1 above), and this requires caveolin-3 trafficking.

There is biochemical evidence that the rapsyn:AChR ratio increases from 1:1 to 2:1 within 40mn of agrin induction (Moransard et al 2003), and another team reported that rapsyn only binds AChR inside caveolin-3 (Zhu et al 2006). Both papers claimed, from biochemistry, that the rapsyn-AChR interaction occurred at clusters. Our data is consistent with these claims in that the rapsyn: AChR ratio increases in a caveolin-3 compartment. However, we argue that this occurs inside t-tubules, not at the cluster.

Our pulse-chased AChR QDT data shows that the level of rapsyn per AChR-QDT increases exactly in accordance with the 40mn plateau proposed by Moransard et al. The first and most obvious reason that this happens inside the cell but not at the

cluster is that immunoflourescent staining shows that rapsyn and AChR slowly increase their density at clusters over hours, but plateau inside the cell within 40mn. We also use exocytic block to show that this association happens inside the cell but not at the cluster.

One thing that could account for the discrepancy in claims is that caveolin-3 t-tubules are very surface accessible. Moransard et al used a surface label, and therefore would have also accessed intracellular compartments that are surface accessible. Also, our high resolution staining of caveolin-3 reveals that it never colocalizes well with clusters and NMJs. Caveolin-3 t-tubules are often very close to clusters but do not overlap well, and the vast majority of caveolin-3 is clearly not at the cluster. T-tubules extend throughout the cell, and are primarily within the bounds of the surface plasma membrane. Hence our data is in agreement with the biochemical data, only we argue that most of the changes happen within the cell, and not at the cluster.

We show that the final state of cluster assembly consists of a high density of AChR and rapsyn density, which is correlated with AChR immobility. This final state of AChR-rapsyn interaction and density occurs intracellularly before insertion at the cluster, and requires caveolin-3 trafficking. There have been a few reports of receptor-scaffold preassembly, this one is novel because we demonstrate how this state of assembly is induced and how it relates to receptor mobility, or stability in the synapse.

It is surprising that t-tubules, a calcium handling organelle, traffic AChRs. Whether a similar process can happen in the CNS is unknown. There are many high fidelity or 'detonator' synapses in the CNS (e.g. mossy fibers and perkinje synapses), and they strongly recruit calcium handling machinery (ER or SA) to their spines (Harris and Weinberg 2012), and express dystroglycan (Satz et al 2010 and Tian et al 1996). Moreover, AMPARs and NMDARs have been found inside these organelles (Racca et al 2000), but how they got there or what they are doing is unknown. Hence it is

possible that a similar trafficking happens in the CNS. However it is very possible that this type of trafficking and packaging has been missed at the CNS for two reasons. The synapses studied in vivo often only have a small percentage of spines with ER (Holbro et al 2009), and ER is sometimes reported not to be recruited to spines in dissociated cultures (Sala et al 2005).

α **Dystroglycan as slot molecule for inserted receptors**.

α Dystroglycan deficient muscle cells in vivo and in vitro form AChR clusters that are described as 'diffuse' (Jacobson et al 2001), which is what we defined as 'weak' (low density of AChR). The mechanism of diffuse or weak cluster formation and lack of strengthening is unknown. Here we propose that α dystroglycan recruits t-tubules, which strengthen clusters by adding AChR-rapsyn packages. I will also discuss how α dystroglycan might further act as a slot molecule for inserted AChR-rapsyn packages, and how it might recruit ER in the CNS.

It is possible that α dystroglycan acts as a slot molecule for inserted receptors but not diffusing receptors. Detubulation allowed α dystroglycan density to increase at the cluster but not AChR and rapsyn (fig 6b). Hence an increase in cluster α dystroglycan alone does not increase AChR to strong levels, even though AChRs are diffusing in the cluster. On the other hand when insertion of packaged receptor occurs, then there is a large immobile fraction of AChRs and an increase in AChR and rapsyn densities. We propose that α dystroglycan recruits t-tubules, which package receptors; and we suggest that α dystroglycan might act as a slot molecule, targeting insertion and anchoring inserted/packaged AChR (fig 3.3).

The dystroglycan complex would qualify as a slot based on its ability to interact and anchor with packaged AChR. We claim that AChRs package with rapsyn and utrophin inside the cell before insertion (fig 5c), and that α dystroglycan is added to

the cluster independently of packaging (fig 6b). Both rapsyn and utrophin interact with the cytoplasmic domain of the dystroglycan complex as well as AChR, and therefore rapsyn and utrophin could anchor AChRs to α dystroglycan (Bartoli et al 2001). α Dystroglycan is likely to be immobile in the synapse, as it is connected to immobile synaptic laminin ECM, and to the cytoskeleton intracellulary. Furthermore the dystroglycan complex is known to signal in cell polarity and adhesion (Batchelor et al 2007), and its signaling could recruit t-tubules to the cluster as well as target exocytic vesicles. This information would lead to the hypotheses that α dystroglycan is the AChR anchor for inserted AChR-rapsyn/utrophin complexes, and that α dystroglycan unbound by AChR-rapsyn signals as an insertion target for AChR-rapsyn packages (fig 3.3).

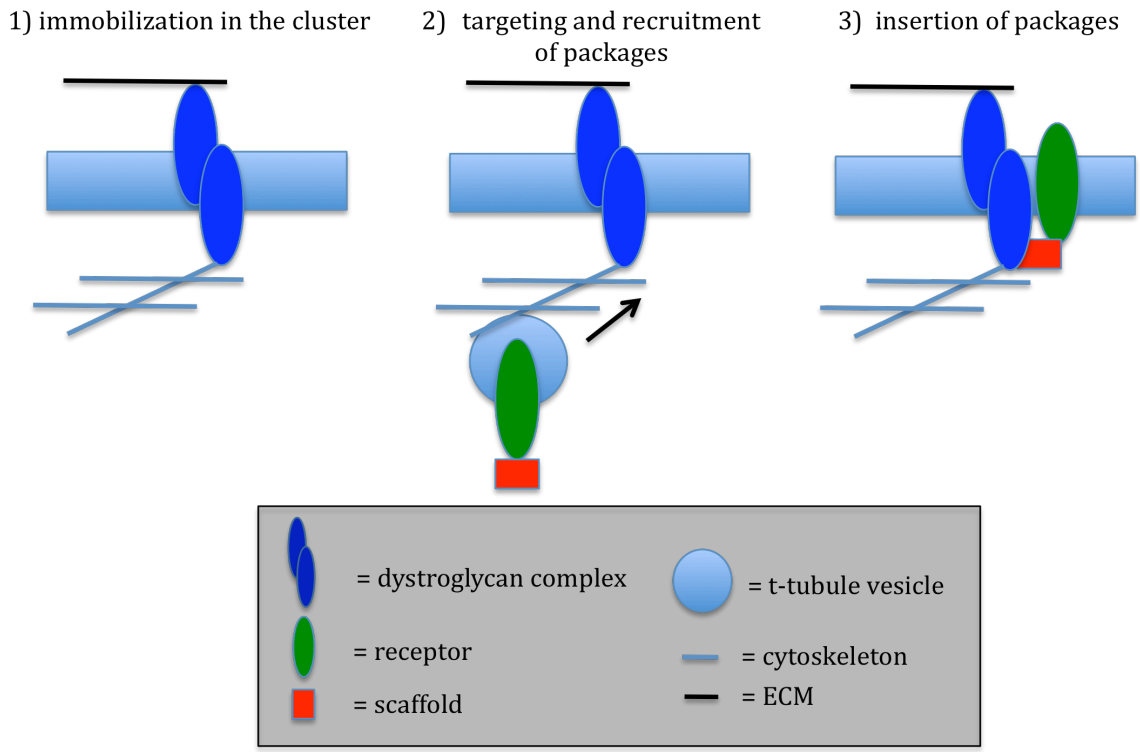

Figure 3.3 The dystroglycan complex as a slot and anchor for AChR.
1)The dystroglycan complex (blue ovoids) would cluster after agrin, but not immobilize diffusing or unpackaged AChR. The dystroglycan complex would immobilize itself by binding ECM as well as the cytoskeleton. 2) Dystroglycan complex signaling recruits t-tubules and targets AChR package insertion. 3) AChR packages insert and interact with dystroglycan via prepackaged scaffold.

If the dystroglycan complex is the anchor for AChRs at the synapse, then by definition it is a slot molecule for AChR (Xu 2011). Therefore, according to the slot model, the number of AChRs added to a strong synapse would be proportional to the number of dystroglycan complexes. Interestingly this seems to be only true for inserted receptors, and not diffusing receptors. Therefore the weak cluster would initially act as diffusion trap, which can trap a limited number of diffusing AChRs but does not immobilize them in a dystroglycan slot. Meanwhile α dystroglycan is also clustered in the trap to form a lattice of slots, which recruit packaged AChr-rapsyn/utrophin for immobile insertion and results in a high density AChR postsynapse. In reference to the previous car park analogy, dytroglycan slots, or parking spaces, would form at the cluster and target the insertion of immobile receptors, but not diffusing receptors. Hence the car park spaces, or slots, would only be permissible to crane mediated parking (insertion), and block normal driving and parking (diffusion).

Aside from it role at the NMJ, α dystroglycan might also recruit calcium handling machinery in the CNS. α Dystroglycan immunoprecipitates with synaptopodin, the molecule best known for recruiting ER to synapses in the CNS. Furthermore, dystroglycan is also expressed in postsynaptic CNS cells that strongly recruit ER (the hippocampal mossy fiber cerebellar purkinje synapses) (Satz et al 2010 and Tian et al 1996). It would be easy to test the role of α dystroglycan in recruiting ER at these synapses by using function blocking antibodies. There are many synapses in CNS which only recruit ER to a subset of spines (e.g hippocampal Ca1 and lateral amygdala)(Holbro et al 2009 and Ostroff et al 2010). It would be interesting to stain for α dystroglycan and see if it correlates with recruited ER in such synapses.

In summary we show that α dystroglycan recruits t-tubules. We propose that a similar mechanism is possible for ER or SA in the CNS, and that dystroglycan is a slot molecule.

In vivo.

The NMJ in vivo strengthens and matures after birth (reviewed in Sanes and Lichtman 2001). AChR stability and density at the NMJ increase after birth (Valenzuela et al 2011); and the rapsyn:AChR ratio increases from 1:1 to 2:1 (Gervasio et al 2007). These in vivo strengthening events are similar to the in vitro t-tubule trafficking and packaging dependent strengthening. Accordingly we find that caveolin-3 t-tubules are heavily recruited to the NMJ at this time, between birth (p0) and NMJ maturation (p20) (fig 7a). We also found that pulse-chased AChRs traffic to caveolin-3 in vivo with a time course similar to in vitro (fig 7b and 3c). Furthermore, AChRs colocalized with rapsyn and Rb27b in vesicles near NMJs as early as p8 (fig 7c). Finally, Rb27b was localized directly above the NMJ, rather than at the periphery suggesting a direct insertion mechanism similar to in vitro.

These data are also in accordance with other in vivo data in the literature. MyosinVa knockdown in muscles causes AChR vesicles to accumulate near the NMJ, and these vesicles are also enriched in rapsyn (Roeder et al 2008). α Dystrolgycan knockdown is embryonic lethal and disruption between dystroglycan and dystrobrevin is used as a mouse model for Duchennes muscular dystrophy (Cote et al 1999). Therefore its role at the NMJ is difficult to interpret in vivo. Our data predict that inhibition of α dystroglycan singaling would allow NMJs to form but not strengthen, and this is exactly what happens in syntrophin knockout mice (Valenzuela et al 2011). Syntrophin binds to the dystroglycan complex cytoplasmicly through dystrobrevin. Syntrophin mice form NMJs that appear normal until after birth, when they fail to increase AChR density and stability at NMJs. In essence this is a very similar result to the detubulation and dytroglycan inhibition experiments in vitro, where NMJs formed but AChR density and stability did not increase (fig 4a, 4d, and 5c). The prediction is that syntrophin mice fail to recruit t-tubules to the NMJ, which could simply be tested by staining for caveolin-3 in these mutant mice. Similarly adding

dystroglycan function blocking antibodies chronically after birth, should yield the same result: NMJs that do not recruit t-tubules nor strengthen.

It is surprising that NMJs in vivo do not recruit t-tubules until after birth because the motor neuron arrives, and the agrin signal starts, at e13. This is in contrast to in vitro where clusters recruit t-tubules over the course of hours after agrin. There are a few reasons that could account for the delay in t-tubule recruitment in vivo. Firstly t-tubule development does not even begin until e15, a few days after NMJ formation (Takekura et al 2001). At this point t-tubules invaginate from the surface membrane and begin formation. Around birth t-tubles begin to properly fill the cell, and they are still longitudinal in orientation, which is the approximate situation of the 5 day old C2C12 myotubes used in our experiments. Full development of t-tubules in vivo coincides roughly with the NMJ's development, a few weeks after birth (reviewed in Al-Qusairi and Laporte 2011). If t-tubules are required for NMJ strengthening, then this late t-tubule development might be sufficient to explain the late increase in AChR density and stability in vivo. Again, syntrophin knockout mice, or dytroglycan inhibition would establish more of a causal role for t-tubules in vivo, similar to that seen in vitro.

Developmentally regulated cleavage of agrin could also explain the delay in AChR density and stability in vivo. After birth, agrin is cleaved at the NMJ by a trypsin protease (Bolliger et al 2010). If this process is inhibited, then AChR density at the NMJ remains low after birth. Hence cleavage of agrin is required for NMJ maturation and increased AChR density. The recombinant agrin added to C2C12 muscles in our in vitro assay is likely to act similarly to the product of cleaved agrin in vivo.

In summary the postnatal strengthening that occurs at NMJs in vivo is likely to be regulated by similar mechanisms that we described in vitro. T-tubule recruitment and trafficking, as well as rapsyn packaging and Rb27b insertion, all correlate with increased AChR stability and density at the NMJ. MyosinVa knockdown in vivo supports our hypothesis that AChR-rapsyn packaging happens inside the cell before

insertion (Roeder et al 2008). Syntrophin knock out mice would establish a causal role for t-tubules in NMJ strengthening if they do not recruit t-tubules.

A role for preassembly-insertion in the CNS?

There is evidence that NMDAR is prepackaged with SAP97 and 102 (Jeyifous et al 2007 and Washbourne et al 200), and that AMPAR is already with stargazin before it arrives at the synapse (Opazo and Choquet 2010). The question is whether these interactions are dynamically regulated, rather than constitutively. At the NMJ, the scaffold molecule rapsyn increases it ratio per AChR after agrin, and a similar increase in ratio is possible between stargazin and Glur1 (Kim et al 2010).

We found that pulse-chased Glur1 increased its colocalization with stargazin inside rhodamine dextran positive vesicles after LTP induction in dissociated hippocampal cells. Furthermore intracellular Glur1 colocalized more strongly with stargazin at the peak of LTP induced exocytosis (20mn). This raises the possibility that Glur1 is increasing its association with stargazin after LTP induction. However a more biochemical approach would be needed to verify an increase in stargazin: glur1 interaction ratio. Nevertheless we used the same increased colocalization by immunostaining to verify the known biochemical increase in rapsyn:AChR. Hence it is quite likely that the increased colocalization reflects an increased association between Glur1 and stargazin.

A mechanism of inserting packaged, immobile receptors could be important in the CNS for larger and stronger synapses, as discussed above. Glur1 has been shown to diffuse into the synapse and become immobile after LTP (Opazo et al 2010), and to be immobile within the PSD (Kerr and Blanpied 2012). Perhaps insertion of immobile Glur1 would be a more efficient mechanism for the sustained addition of immobile receptors at a strengthened synapse. Furthermore activation of the ER organelle and the adhesion molecules which recruit it, rather than just potentiating the synapse, could be a useful way to tag a synapse. A continuous and potentiated

ER spanning multiple spines could also explain how plasticity is clustered to neighboring spines when only one spine is potentiated (Harvery and Svoboda 2007). This is a plausible mechanism because large spines, such as those seen in clustered plasticity, often contain ER, and ER is often found in stable spines induced by learning in vivo (Knott et al 2006). Hence ER could signal a long way inside the neuron, to neighbouring synapses, or even back to the cell body.

An ER based mechanism would also be interesting for outside-in regulation. We found that adhesion regulates t-tubules, hence a secreted protease which alters adhesion could have perisynaptic, outside-in regulation of ER during clustered plasticity. Our results show the induced regulation of t-tubules (a calcium handling, ER associated organelle) in postsynaptic strengthening, and it will be very interesting to see if this mechanism generalizes to the CNS.

The idea that postsynaptic receptor stability can be regulated inside the cell, rather than at the synapse, is conceptually novel. It has widely been assumed that synaptic strength is regulated locally at the synapse, in situ. A preassemble-insert model would allow synaptic strength to be regulated inside the cell at a distance from the synapse. This would imply that the state of the cell influences the strength of its synapses (ER could be blocked from packaging, not recruited to the dendrite, a cluster of synapses, or an individual synapse), which might be an important process in homeostatic, clustered, and single synapse plasticity, as well as disease.

This study is the first to report prepackaging of receptor-scaffold complexes and insertion of immobile packages. Surprisingly we find that prepackaging is induced by agrin and regulated by t-tubules, a calcium handling organelle that associates with ER. In many cases the exact same or analogous cellular and molecular machinery is in place at the CNS to accomplish the same mechanism: dystroglycan interacts with synaptopodin and is localized at strong synapses loaded with ER; NMDAR and AMPAR have mysteriously been found in ER in spines; and scaffold molecules might increase their ratio per receptor. The role of spine ER in synaptic

strengthening is still mysterious and the possibility that they regulate prepacking and receptor stability at the synapse is intriguing. Furthermore the idea of potentiating an intracellular organelle, which can propagate signals over a longer distance and beyond the locale of the synapse is particularly exciting for synaptic tagging and clustered plasticity. We also propose that direct insertion of immobile receptors is an efficient way to add protein to any cell-cell junction that is impermeable to diffusion or has a high immobile fraction.

Finally, the original data for the diffusion-trap model originated from AChR clustering, and has since been verified at many synapses. AChR clustering in myotubes has been a very robust and faithful model. Therefore it is plausible that a preassemble-insert model regulated by ER and calcium handling organelles will have relevance to a variety of synapses and cell-cell contacts.

Methods and Materials.

C2C12 cell culture, Agrin cluster induction, APOE4 and anti-dystroglycan treatments, Detubulation, NEM, and MyosinVa knockdown.

C2C12 myoblasts, from the European Collection of Cell Cultures (ECACC), were passaged in DMEM + 10% FBS (Gibco)(growth medium (GM)). Myoblasts were grown to 80% confluency in GM and then differentiated into myotubes in DMEM with 2% horse serum (Gibco), and 2mM l-glutamine (differentiating medium (DM)). Cells were incubated at 37C in 5% CO2 and 95% humidity and plated on either 35mm or 8 well tissue culture ibidi imaging dishes (Vitaris). Agrin clusters were induced by the bath addition of recombinant purified rat agrin 50ng/ml (RnD systems 550-AG), in DM, to day 5-7 myotubes.

Cells were pretreated with APOE4 (cell science CRA404A) at a molar ratio 5x to agrin (250ng/ml) for 5mn, before the addition of agrin. Cells were not washed after treatment to ensure the presence of APOE4 and agrin. Similarly cells were pretreated with anti- α dystroglycan 2H6C4 (1:100).

For detubulation cells were treated with 300mM glycine in cold (4C) PBS- for 2mn. Cells were then washed 3x with room temperature medium, and then agrin was added at 37C.

NEM was diluted in DMSO and into DM at a final concentration of 50nM (Zhu et al 2006). NEM-DM was added to cells after 2hrs agrin, during the insertion experiments, and after the labeling.

MyosinVa was knocked down in cells using the Sigma Mission lentiviral transduction particle system. Lentiviral transduction particles were purchased at 1.8x107 TU/ml, in 200ul, and 10ul were used per well (in ibidi 8 well), in 250ul DM.

The clone used was verified by Sigma, (TRCN000011963, NM_172668). Knockdowns were verified in cells by posthoc staining for myosinVA, and cells with little knockdown were used as controls.

Primary Neuronal cell culture, live cell GluR1 labeling, and glycine stimulation.

Primary hippocampal cultures were prepared from Sprague-Dawley rats, on 8 well ibidi tissue culture dishes. Briefly, hippocampi were dissected from e18 rat embryos, and kept in cold HBSS until dissociation with 0.1% trypsin-EDTA (gibco) for 5-10mn, after which cells were kept in DMEM + 10% FBS. Debris was filtered with nylon paper, and cells were plated at 70,000 cells per well (approximately $1cm^2$). Cells were left to adhere for atleast an hour before switching the media to neurobasal medium supplemented with 1x B27 and glutamax (Invitrogen). Cells for experiments were grown to DIV18-21, a time when synapses are mature. NMDAR dependent LTP was mimicked by adding 200um glycine, to activate NMDAR, for 5mn (Park et al 2006).

Glur1 was labeled with an anti N-terminal monoclonal (Rh95, Millipore) at 1:50, after cells were cooled to 4C for 5mn. Cells were then washed in PBS, before glycine stimulation. Where relevant rhodamine dextran (10kd mw, Invitrogen) was added for 5mn after glycine stimulation. To label intracellular GluR1the surface was labeled as above for 10mn. Cells were then washed, fixed without permeabilization, and then stained for anti-Glur1 to label all surface molecules. Cells were then permeabilized with triton and stained for intracellular Glur1 with the same antibody.

Fixation and staining.

Myotubes and hippocampal cultures were fixed with room temperature 4% paraformaldehyde in PBS- for 8mn, and then for additional 8mn with 4%

paraformaldehyde plus 0.1% triton. Cells were washed and then blocked with 2.5%BSA. Primary antibody labeling was in block over night at 4C, and secondary labeling was for 2hrs (1:1000) at room temperature.

Muscles were dissected and fixed in 4%paraformaldhyde for 1hr. They were then sucrose (30%) treated and embedded in OCT for freezing. 20um sections were cut, and then post fixed with 4% paraformaldehyde and 1% triton for 30mn. Primary and secondary staining was the same as above.

Labeling live cells: insertion assay and QDT labeling.

For the insertion assay, myotubes were cooled to 4C for 5mn, and then BTX488 was added (1:333) for 10mn at 4C. After washing 5x with room temperature PBS-, BTX555 (1:1000) was added to the bath for 40mn. Images were acquired every 10mn during insertion in live cells, or fixed and stained at different times after agrin.

To label AChRs with QDTs , BTX-biotin stock (as per manufacturers instructions (500ug/500ul) was diluted 1:500, and stock BTX-555 was diluted 1:333 in separate tubes. 100ul of diluted BTX-biotin was then diluted into BTX-555, with end concentrations of BTX-Biotin 1:5000, and BTX-555 1:333, in 1ml DMEM. This way receptors were sparsely labeled with BTX-biotin and mostly BTX-555, in order to ensure sparse QDT labeling later and to reduce the chance of cross-linking after adding streptavidin-QDTs. Myotubes were then labeled for 2mn at 4C with BTX-biotin and BTX-555 in DM. Cells were washed 5x, and then 1ul (of 1uM stock QDT solution) was added to 1ml DM to label cells at 4C for 2mn. Cells were then washed 8x with room temperature DM, before imaging. For ex vivo QDT labeling the same protocol was followed on dissected diaphragms which were treated with .2mg/ml collagenase for 1mn, before labeling, and the duration of labeling times were doubled.

Antibodies (list and dilutions).

Caveolin-3 monoclonal (1:5000)

Dysferlin rabbit polyclonal (abcam 15108)

mtm1 goat polyclonal (Santacruz) (1:100)

Rab4,5,11, BD transduction labs (1:200)

Rab6,7,9,27a Santacruz (1:200)

Rapsyn monoclonal 1234 (abcam 11423) (1:200)

Bungarotoxin conjugated to alexafluor-448, -555 or biotin (invitrogen, diluted to manufacturers instructions 1ug/ul PBS) used at 1:1000 in fixed cells, and 1:333 in live cells.

Utrophin monoclonal (BD transduction labs 610896) (1:1000).

α Dystroglycan monoclonal 2H6C4 Millipore. Function blocking at 1ul per 100ul media, staining at 1:1000.

Myosin Va (LF-18) rabbit polyclonal (Sigma, M 4812)

Anti-GluR1-NT, clone RH95, Millipore. Surface labeling at 2ul per 100ul media, or 1:1000 in fixed cells.

Stargazin rabbit polyclonal ab9876 Millipore (1:300).

Alexaflours (Invitrogen) for corresponding animals were used as secondary antibodies.

Streptavidin coated quantumdot 655 was purchased from Invitrogen

4 Dimensional live-cell microscopy and FRAP.

Myoblasts were differentiated into myotubes on 35mm Ibidi tissue culture dishes. 5 to 7 day old myotubes were labeled with Alexa Fluor conjugated bungarotoxin (Invitrogen), for 10mns at 37°C. Cells were then washed three times in warm differentiating media without phenol red. 750ul of DMEM without phenol red (to reduce autofluorescence) was then added to the dish. The dish was immediately placed on a heated stage with 5% CO2 controlled atmosphere, and imaged before the addition of agrin. Immediately after, agrin was added to the dish and then cells

were imaged every 20 minutes for 6 hours and then every 1.5 hours overnight on a Zeiss Till5 longrun, 60x oil immersion objective with 1.4NA, and run with Metamorph software. An EMCCD camera was used to collect signal. Experiments were also repeated at 0,45mn, 3hr and 6hr on a Zeiss LSM, with a 60x 1.3NA oil immersion. Z-stacks were taken by imaging every 0.5um in z, from top to bottom of cell. Images were deconvoluted with Huygens software and three dimensionally reconstructed in Imaris. In some cases cells were fixed and stained post hoc at the microscope.

To bleach clusters, cells were labeled as before for live cell imaging with BTX-488, at different times after agrin. Regions of interest surrounding the clusters were defined with Zeiss software and then bleached with 100% laser power. Images were acquired immediately before and after bleaching, and then at relevant time-points afterwards. Non-bleached clusters were used to control for bleaching caused by imaging.

Single molecule optical microscopy and tracking.

Cells were imaged at 37C in an 35mm ibidi dish, under 5% $C0_2$ and humidified conditions, on a zeiss spinning disc microscope, using a 100x 1.45NA objective. Quantum dots were excited by a 445nm laser, and a longpass filter was used to collect emmision over 560nm, to image QDT655. BTX-555 was used to locate clusters, and was imaged with standard RGB excitation laser and filters. Clusters were imaged before and after each QDT imaging, to account for mechanical drift and to ensure that focus remained on the cluster. In some instance the cluster and quantum dot were imaged simultaneously. QDTs were imaged with an integration time of 50ms for three minutes, or with 100ms exposure every second for up to 20 minutes. Signals were recorded with an EMCCD camera.

AChR-QDT tracks were made with an Imaris tracking program after images were run through a Guassian filter. Tracks with 75 consecutive frames with no more than

3 gaps or blinks were used for analysis. Mean square displacement and diffusion coefficients were calculated using a homemade matlab program running on Imaris, which was largely based on Opazo et al 2010 and Bannai et al 2009. QDTs tracks within clusters were defined by overlaying the track with the cluster image taken before and after the acquisition. Diffusion coefficients were calculated inside the clusters. Immobility was defined by tracks that did not exceed the radius of the QDT signal, or by a diffusion coefficient of less than 0.005 um^2/s. Immobility was also verified by imaging every second over the course of minutes. The frequency of AChR-QDTs diffusing into clusters was calculated by the number of times QDTS diffused from outside to inside the cluster per experiment.

Statistics.

T-tests and ANOVAs were run with graphpad software, and error bars represent SEMs. Stars are used to denote significance, where one star idicates a p-value less than 0.05, two stars less than 0.005, and three stars less than 0.0005.

References.

Adams, C.L., Chen, Y.T., Smith, S.J., and Nelson, W.J. (1998). Mechanisms of epithelial cell-cell adhesion and cell compaction revealed by high-resolution tracking of E-cadherin-green fluorescent protein. The Journal of cell biology *142*, 1105-1119.

Al-Qusairi, L., and Laporte, J. (2011). T-tubule biogenesis and triad formation in skeletal muscle and implication in human diseases. Skeletal muscle *1*, 26.

Axelrod, D., Ravdin, P., Koppel, D.E., Schlessinger, J., Webb, W.W., Elson, E.L., and Podleski, T.R. (1976). Lateral motion of fluorescently labeled acetylcholine receptors in membranes of developing muscle fibers. Proceedings of the National Academy of Sciences of the United States of America *73*, 4594-4598.

Bannai, H., Levi, S., Schweizer, C., Inoue, T., Launey, T., Racine, V., Sibarita, J.B., Mikoshiba, K., and Triller, A. (2009). Activity-dependent tuning of inhibitory neurotransmission based on GABAAR diffusion dynamics. Neuron *62*, 670-682.

Bartoli, M., Ramarao, M.K., and Cohen, J.B. (2001). Interactions of the rapsyn RING-H2 domain with dystroglycan. The Journal of biological chemistry *276*, 24911-24917.

Bas Orth, C., Vlachos, A., Del Turco, D., Burbach, G.J., Haas, C.A., Mundel, P., Feng, G., Frotscher, M., and Deller, T. (2005). Lamina-specific distribution of Synaptopodin, an actin-associated molecule essential for the spine apparatus, in identified principal cell dendrites of the mouse hippocampus. The Journal of comparative neurology *487*, 227-239.

Batchelor, C.L., Higginson, J.R., Chen, Y.J., Vanni, C., Eva, A., and Winder, S.J. (2007). Recruitment of Dbl by ezrin and dystroglycan drives membrane proximal Cdc42 activation and filopodia formation. Cell Cycle *6*, 353-363.

Bolliger, M.F., Zurlinden, A., Luscher, D., Butikofer, L., Shakhova, O., Francolini, M., Kozlov, S.V., Cinelli, P., Stephan, A., Kistler, A.D*., et al.* (2010). Specific proteolytic cleavage of agrin regulates maturation of the neuromuscular junction. Journal of cell science *123*, 3944-3955.

Bruneau, E.G., Macpherson, P.C., Goldman, D., Hume, R.I., and Akaaboune, M. (2005). The effect of agrin and laminin on acetylcholine receptor dynamics in vitro. Developmental biology *288*, 248-258.

Bu, G. (2009). Apolipoprotein E and its receptors in Alzheimer's disease: pathways, pathogenesis and therapy. Nature reviews Neuroscience *10*, 333-344.

Cao, C., Backer, J.M., Laporte, J., Bedrick, E.J., and Wandinger-Ness, A. (2008). Sequential actions of myotubularin lipid phosphatases regulate endosomal PI(3)P and growth factor receptor trafficking. Molecular biology of the cell *19*, 3334-3346.

Cartaud, A., Coutant, S., Petrucci, T.C., and Cartaud, J. (1998). Evidence for in situ and in vitro association between beta-dystroglycan and the subsynaptic 43K rapsyn protein. Consequence for acetylcholine receptor clustering at the synapse. The Journal of biological chemistry *273*, 11321-11326.

Causeret, M., Taulet, N., Comunale, F., Favard, C., and Gauthier-Rouviere, C. (2005). N-cadherin association with lipid rafts regulates its dynamic assembly at cell-cell junctions in C2C12 myoblasts. Molecular biology of the cell *16*, 2168-2180.

Comley, L.H., Fuller, H.R., Wishart, T.M., Mutsaers, C.A., Thomson, D., Wright, A.K., Ribchester, R.R., Morris, G.E., Parson, S.H., Horsburgh, K.*, et al.* (2011). ApoE isoform-specific regulation of regeneration in the peripheral nervous system. Human molecular genetics *20*, 2406-2421.

Cote, P.D., Moukhles, H., Lindenbaum, M., and Carbonetto, S. (1999). Chimaeric mice deficient in dystroglycans develop muscular dystrophy and have disrupted myoneural synapses. Nature genetics *23*, 338-342.

DeChiara, T.M., Bowen, D.C., Valenzuela, D.M., Simmons, M.V., Poueymirou, W.T., Thomas, S., Kinetz, E., Compton, D.L., Rojas, E., Park, J.S.*, et al.* (1996). The receptor tyrosine kinase MuSK is required for neuromuscular junction formation in vivo. Cell *85*, 501-512.

Deller, T., Korte, M., Chabanis, S., Drakew, A., Schwegler, H., Stefani, G.G., Zuniga, A., Schwarz, K., Bonhoeffer, T., Zeller, R.*, et al.* (2003). Synaptopodin-deficient mice lack a spine apparatus and show deficits in synaptic plasticity. Proceedings of the National Academy of Sciences of the United States of America *100*, 10494-10499.

Dubinsky, J.M., Loftus, D.J., Fischbach, G.D., and Elson, E.L. (1989). Formation of acetylcholine receptor clusters in chick myotubes: migration or new insertion? The Journal of cell biology *109*, 1733-1743.

Ehrensperger, M.V., Hanus, C., Vannier, C., Triller, A., and Dahan, M. (2007). Multiple association states between glycine receptors and gephyrin identified by SPT analysis. Biophysical journal *92*, 3706-3718.

Gee, S.H., Montanaro, F., Lindenbaum, M.H., and Carbonetto, S. (1994). Dystroglycan-alpha, a dystrophin-associated glycoprotein, is a functional agrin receptor. Cell *77*, 675-686.

Gervasio, O.L., Armson, P.F., and Phillips, W.D. (2007). Developmental increase in the amount of rapsyn per acetylcholine receptor promotes postsynaptic receptor packing and stability. Developmental biology *305*, 262-275.

Gervasio, O.L., and Phillips, W.D. (2005). Increased ratio of rapsyn to ACh receptor stabilizes postsynaptic receptors at the mouse neuromuscular synapse. The Journal of physiology *562*, 673-685.

Glass, D.J., Bowen, D.C., Stitt, T.N., Radziejewski, C., Bruno, J., Ryan, T.E., Gies, D.R., Shah, S., Mattsson, K., Burden, S.J.*, et al.* (1996). Agrin acts via a MuSK receptor complex. Cell *85*, 513-523.

Glover, L., and Brown, R.H., Jr. (2007). Dysferlin in membrane trafficking and patch repair. Traffic *8*, 785-794.

Harris, K.M., and Weinberg, R.J. (2012). Ultrastructure of synapses in the Mammalian brain. Cold Spring Harbor perspectives in biology *4*. doi: 10.1101/cshperspect.a005587

Harvey, C.D., and Svoboda, K. (2007). Locally dynamic synaptic learning rules in pyramidal neuron dendrites. Nature *450*, 1195-1200.

Hezel, M., de Groat, W.C., and Galbiati, F. (2010). Caveolin-3 promotes nicotinic acetylcholine receptor clustering and regulates neuromuscular junction activity. Molecular biology of the cell *21*, 302-310.

Holbro, N., Grunditz, A., and Oertner, T.G. (2009). Differential distribution of endoplasmic reticulum controls metabotropic signaling and plasticity at hippocampal synapses. Proceedings of the National Academy of Sciences of the United States of America *106*, 15055-15060.

Holtmaat, A., Wilbrecht, L., Knott, G.W., Welker, E., and Svoboda, K. (2006). Experience-dependent and cell-type-specific spine growth in the neocortex. Nature *441*, 979-983.

Hu, Q., Milenkovic, L., Jin, H., Scott, M.P., Nachury, M.V., Spiliotis, E.T., and Nelson, W.J. (2010). A septin diffusion barrier at the base of the primary cilium maintains ciliary membrane protein distribution. Science *329*, 436-439.

Jacob, T.C., Bogdanov, Y.D., Magnus, C., Saliba, R.S., Kittler, J.T., Haydon, P.G., and Moss, S.J. (2005). Gephyrin regulates the cell surface dynamics of synaptic GABAA receptors. The Journal of neuroscience : the official journal of the Society for Neuroscience *25*, 10469-10478.

Jacobson, C., Cote, P.D., Rossi, S.G., Rotundo, R.L., and Carbonetto, S. (2001). The dystroglycan complex is necessary for stabilization of acetylcholine receptor clusters at neuromuscular junctions and formation of the synaptic basement membrane. The Journal of cell biology *152*, 435-450.

Jedlicka, P., Schwarzacher, S.W., Winkels, R., Kienzler, F., Frotscher, M., Bramham, C.R., Schultz, C., Bas Orth, C., and Deller, T. (2009). Impairment of in vivo theta-burst long-term potentiation and network excitability in the dentate gyrus of synaptopodin-deficient mice lacking the spine apparatus and the cisternal organelle. Hippocampus *19*, 130-140.

Jeyifous, O., Waites, C.L., Specht, C.G., Fujisawa, S., Schubert, M., Lin, E.I., Marshall, J., Aoki, C., de Silva, T., Montgomery, J.M*., et al.* (2009). SAP97 and CASK mediate sorting of NMDA receptors through a previously unknown secretory pathway. Nature neuroscience *12*, 1011-1019.

Jordan, K., Solan, J.L., Dominguez, M., Sia, M., Hand, A., Lampe, P.D., and Laird, D.W. (1999). Trafficking, assembly, and function of a connexin43-green fluorescent protein chimera in live mammalian cells. Molecular biology of the cell *10*, 2033-2050.

Kennedy, M.J., Davison, I.G., Robinson, C.G., and Ehlers, M.D. (2010). Syntaxin-4 defines a domain for activity-dependent exocytosis in dendritic spines. Cell *141*, 524-535.

Kerr, M.J., Blanpied ,T.A., I.G. (2012). Subsynaptic AMPA receptor distribution is acutely regulated by actin-driven reorganization of the postsynaptic density. The Journal of Neurosceince *32(2)*, 658-673.

Kim, K.S., Yan, D., and Tomita, S. (2010). Assembly and stoichiometry of the AMPA receptor and transmembrane AMPA receptor regulatory protein complex. The Journal of neuroscience : the official journal of the Society for Neuroscience *30*, 1064-1072.

Kim, N., Stiegler, A.L., Cameron, T.O., Hallock, P.T., Gomez, A.M., Huang, J.H., Hubbard, S.R., Dustin, M.L., and Burden, S.J. (2008). Lrp4 is a receptor for Agrin and forms a complex with MuSK. Cell *135*, 334-342.

Knott, G.W., Holtmaat, A., Wilbrecht, L., Welker, E., and Svoboda, K. (2006). Spine growth precedes synapse formation in the adult neocortex in vivo. Nature neuroscience *9*, 1117-1124.

Kucharz, K., Krogh, M., Ng, A.N., and Toresson, H. (2009). NMDA receptor stimulation induces reversible fission of the neuronal endoplasmic reticulum. PloS one *4*, e5250.
Kummer, T.T., Misgeld, T., and Sanes, J.R. (2006). Assembly of the postsynaptic membrane at the neuromuscular junction: paradigm lost. Current opinion in neurobiology *16*, 74-82.

Lee, C.W., Han, J., Bamburg, J.R., Han, L., Lynn, R., and Zheng, J.Q. (2009). Regulation of acetylcholine receptor clustering by ADF/cofilin-directed vesicular trafficking. Nature neuroscience *12*, 848-856.

Levi, S., Schweizer, C., Bannai, H., Pascual, O., Charrier, C., and Triller, A. (2008). Homeostatic regulation of synaptic GlyR numbers driven by lateral diffusion. Neuron *59*, 261-273.

Makino, H., and Malinow, R. (2009). AMPA receptor incorporation into synapses during LTP: the role of lateral movement and exocytosis. Neuron *64*, 381-390.

Martinez-Pena y Valenzuela, I., Mouslim, C., Pires-Oliveira, M., Adams, M.E., Froehner, S.C., and Akaaboune, M. (2011). Nicotinic acetylcholine receptor stability at the NMJ deficient in alpha-syntrophin in vivo. The Journal of neuroscience : the official journal of the Society for Neuroscience *31*, 15586-15596.

Martone, M.E., Zhang, Y., Simpliciano, V.M., Carragher, B.O., and Ellisman, M.H. (1993). Three-dimensional visualization of the smooth endoplasmic reticulum in Purkinje cell dendrites. The Journal of neuroscience : the official journal of the Society for Neuroscience *13*, 4636-4646.

McAllister, A.K. (2007). Dynamic aspects of CNS synapse formation. Annual review of neuroscience *30*, 425-450.

McMahan, U.J. (1990). The agrin hypothesis. Cold Spring Harbor symposia on quantitative biology *55*, 407-418.

Mittaud, P., Marangi, P.A., Erb-Vogtli, S., and Fuhrer, C. (2001). Agrin-induced activation of acetylcholine receptor-bound Src family kinases requires Rapsyn and correlates with acetylcholine receptor clustering. The Journal of biological chemistry *276*, 14505-14513.

Moransard, M., Borges, L.S., Willmann, R., Marangi, P.A., Brenner, H.R., Ferns, M.J., and Fuhrer, C. (2003). Agrin regulates rapsyn interaction with surface acetylcholine receptors, and this underlies cytoskeletal anchoring and clustering. The Journal of biological chemistry *278*, 7350-7359.

Nachury, M.V., Seeley, E.S., and Jin, H. (2010). Trafficking to the ciliary membrane: how to get across the periciliary diffusion barrier? Annual review of cell and developmental biology *26*, 59-87.

Opazo, P., and Choquet, D. (2011). A three-step model for the synaptic recruitment of AMPA receptors. Molecular and cellular neurosciences *46*, 1-8.

Opazo, P., Labrecque, S., Tigaret, C.M., Frouin, A., Wiseman, P.W., De Koninck, P., and Choquet, D. (2010). CaMKII triggers the diffusional trapping of surface AMPARs through phosphorylation of stargazin. Neuron *67*, 239-252.

Ostroff, L.E., Cain, C.K., Bedont, J., Monfils, M.H., and Ledoux, J.E. (2010). Fear and safety learning differentially affect synapse size and dendritic translation in the lateral amygdala. Proceedings of the National Academy of Sciences of the United States of America *107*, 9418-9423.

Passafaro, M., Piech, V., and Sheng, M. (2001). Subunit-specific temporal and spatial patterns of AMPA receptor exocytosis in hippocampal neurons. Nature neuroscience *4*, 917-926.

Patrie, K.M., Drescher, A.J., Welihinda, A., Mundel, P., and Margolis, B. (2002). Interaction of two actin-binding proteins, synaptopodin and alpha-actinin-4, with the tight junction protein MAGI-1. The Journal of biological chemistry *277*, 30183-30190.

Patterson, M.A., Szatmari, E.M., and Yasuda, R. (2010). AMPA receptors are exocytosed in stimulated spines and adjacent dendrites in a Ras-ERK-dependent manner during long-term potentiation. Proceedings of the National Academy of Sciences of the United States of America *107*, 15951-15956.

Racca, C., Stephenson, F.A., Streit, P., Roberts, J.D., and Somogyi, P. (2000). NMDA receptor content of synapses in stratum radiatum of the hippocampal CA1 area. The Journal of neuroscience : the official journal of the Society for Neuroscience *20*, 2512-2522.

Ramirez, O.A., and Couve, A. (2011). The endoplasmic reticulum and protein trafficking in dendrites and axons. Trends in cell biology *21*, 219-227.

Rasband, M.N. (2010). The axon initial segment and the maintenance of neuronal polarity. Nature reviews Neuroscience *11*, 552-562.

Renner, M., Specht, C.G., and Triller, A. (2008). Molecular dynamics of postsynaptic receptors and scaffold proteins. Current opinion in neurobiology *18*, 532-540.

Roder, I.V., Petersen, Y., Choi, K.R., Witzemann, V., Hammer, J.A., 3rd, and Rudolf, R. (2008). Role of Myosin Va in the plasticity of the vertebrate neuromuscular junction in vivo. PloS one *3*, e3871.

Ruegg, M.A., Tsim, K.W., Horton, S.E., Kroger, S., Escher, G., Gensch, E.M., and McMahan, U.J. (1992). The agrin gene codes for a family of basal lamina proteins that differ in function and distribution. Neuron *8*, 691-699.

Ryan, T.A., Myers, J., Holowka, D., Baird, B., and Webb, W.W. (1988). Molecular crowding on the cell surface. Science *239*, 61-64.

Sala, C., Roussignol, G., Meldolesi, J., and Fagni, L. (2005). Key role of the postsynaptic density scaffold proteins Shank and Homer in the functional architecture of Ca2+ homeostasis at dendritic spines in hippocampal neurons. The Journal of neuroscience : the official journal of the Society for Neuroscience *25*, 4587-4592.

Sanes, J.R., and Lichtman, J.W. (2001). Induction, assembly, maturation and maintenance of a postsynaptic apparatus. Nature reviews Neuroscience *2*, 791-805.

Sans, N., Prybylowski, K., Petralia, R.S., Chang, K., Wang, Y.X., Racca, C., Vicini, S., and Wenthold, R.J. (2003). NMDA receptor trafficking through an interaction between PDZ proteins and the exocyst complex. Nature cell biology *5*, 520-530.

Satz, J.S., Ostendorf, A.P., Hou, S., Turner, A., Kusano, H., Lee, J.C., Turk, R., Nguyen, H., Ross-Barta, S.E., Westra, S.*, et al.* (2010). Distinct functions of glial and neuronal dystroglycan in the developing and adult mouse brain. The Journal of neuroscience : the official journal of the Society for Neuroscience *30*, 14560-14572.

Shafrir, Y., ben-Avraham, D., and Forgacs, G. (2000). Trafficking and signaling through the cytoskeleton: a specific mechanism. Journal of cell science *113 (Pt 15)*, 2747-2757.

Shaw, R.M., Fay, A.J., Puthenveedu, M.A., von Zastrow, M., Jan, Y.N., and Jan, L.Y. (2007). Microtubule plus-end-tracking proteins target gap junctions directly from the cell interior to adherens junctions. Cell *128*, 547-560.

Sheng, M., and Hoogenraad, C.C. (2007). The postsynaptic architecture of excitatory synapses: a more quantitative view. Annual review of biochemistry *76*, 823-847.

Shi, Y., Lu, W., Milstein, A.D., and Nicoll, R.A. (2009). The stoichiometry of AMPA receptors and TARPs varies by neuronal cell type. Neuron *62*, 633-640.

Simek, J., Churko, J., Shao, Q., and Laird, D.W. (2009). Cx43 has distinct mobility within plasma-membrane domains, indicative of progressive formation of gap-junction plaques. Journal of cell science *122*, 554-562.

Sprague, B.L., and McNally, J.G. (2005). FRAP analysis of binding: proper and fitting. Trends in cell biology *15*, 84-91.

Stein, M.P., Dong, J., and Wandinger-Ness, A. (2003). Rab proteins and endocytic trafficking: potential targets for therapeutic intervention. Advanced drug delivery reviews *55*, 1421-1437.

Stetzkowski-Marden, F., Gaus, K., Recouvreur, M., Cartaud, A., and Cartaud, J. (2006). Agrin elicits membrane lipid condensation at sites of acetylcholine receptor clusters in C2C12 myotubes. Journal of lipid research *47*, 2121-2133.

Sytnyk, V., Leshchyns'ka, I., Delling, M., Dityateva, G., Dityatev, A., and Schachner, M. (2002). Neural cell adhesion molecule promotes accumulation of TGN organelles at sites of neuron-to-neuron contacts. The Journal of cell biology *159*, 649-661.

Takekura, H., Flucher, B.E., and Franzini-Armstrong, C. (2001). Sequential docking, molecular differentiation, and positioning of T-Tubule/SR junctions in developing mouse skeletal muscle. Developmental biology *239*, 204-214.

Tardin, C., Cognet, L., Bats, C., Lounis, B., and Choquet, D. (2003). Direct imaging of lateral movements of AMPA receptors inside synapses. The EMBO journal *22*, 4656-4665.

Tian, M., Jacobson, C., Gee, S.H., Campbell, K.P., Carbonetto, S., and Jucker, M. (1996). Dystroglycan in the cerebellum is a laminin alpha 2-chain binding protein at the glial-vascular interface and is expressed in Purkinje cells. The European journal of neuroscience *8*, 2739-2747.

Triller, A., and Choquet, D. (2003). Synaptic structure and diffusion dynamics of synaptic receptors. Biology of the cell / under the auspices of the European Cell Biology Organization *95*, 465-476.

Triller, A., and Choquet, D. (2008). New concepts in synaptic biology derived from single-molecule imaging. Neuron *59*, 359-374.

Washbourne, P., Bennett, J.E., and McAllister, A.K. (2002). Rapid recruitment of NMDA receptor transport packets to nascent synapses. Nature neuroscience *5*, 751-759.

Willig, K.I., Rizzoli, S.O., Westphal, V., Jahn, R., and Hell, S.W. (2006). STED microscopy reveals that synaptotagmin remains clustered after synaptic vesicle exocytosis. Nature *440*, 935-939.

Wisco, D., Anderson, E.D., Chang, M.C., Norden, C., Boiko, T., Folsch, H., and Winckler, B. (2003). Uncovering multiple axonal targeting pathways in hippocampal neurons. The Journal of cell biology *162*, 1317-1328.

Wu, H., Xiong, W.C., and Mei, L. (2010). To build a synapse: signaling pathways in neuromuscular junction assembly. Development *137*, 1017-1033.

Xu, W. (2011). PSD-95-like membrane associated guanylate kinases (PSD-MAGUKs) and synaptic plasticity. Current opinion in neurobiology *21*, 306-312.

Yudowski, G.A., Puthenveedu, M.A., Leonoudakis, D., Panicker, S., Thorn, K.S., Beattie, E.C., and von Zastrow, M. (2007). Real-time imaging of discrete exocytic events mediating surface delivery of AMPA receptors. The Journal of neuroscience: the official journal of the Society for Neuroscience *27*, 11112-11121.

Zhang, B., Luo, S., Wang, Q., Suzuki, T., Xiong, W.C., and Mei, L. (2008). LRP4 serves as a coreceptor of agrin. Neuron *60*, 285-297.

Zhu, D., Xiong, W.C., and Mei, L. (2006). Lipid rafts serve as a signaling platform for nicotinic acetylcholine receptor clustering. The Journal of neuroscience : the official journal of the Society for Neuroscience *26*, 4841-4851.

Zhu, D., Yang, Z., Luo, Z., Luo, S., Xiong, W.C., and Mei, L. (2008). Muscle-specific receptor tyrosine kinase endocytosis in acetylcholine receptor clustering in response to agrin. The Journal of neuroscience : the official journal of the Society for Neuroscience *28*, 1688-1696.